"Back" to the Future: An Evaluation of Morphological Integration in Kyphosis

2018

Kristyna L. Ceuninck
University of Central Florida

“Back” to the Future: An Evaluation of Morphological Integration in Kyphosis

by

KRISTYNA CEUNINCK

A thesis submitted in partial fulfillment of the requirements

for the Honors in the Major Program in Anthropology

and in the College of Sciences

and in the Burnett Honors College

at the University of Central Florida

Orlando, Florida

Spring Term, 2018

Thesis Chair: John Starbuck, Ph.D.

Abstract

Morphological integration refers to the interdependence of two or more phenotypic structures. The morphological integration concept is based on the fact that parts of complex organisms do not vary randomly and instead display degrees of non-independence that are thought to occur from shared genetic or developmental origins, and/or functional demands. Integrated traits may develop, evolve, and be inherited together. One instance of morphological integration can be found between the vertebral column and the skull. Due to the position of the skull resting atop of the vertebral column, posture may influence skull development and overall craniofacial morphology. Morphological integration within or between structures is typically statistically assessed by exploring correlation and covariation patterns among biological structures of interest. In this study, an analysis of morphological integration was carried out by studying covariation of morphometric measures from the vertebral column and craniofacial complex. Age- and sex-matched, de-identified computed tomography images of individuals with kyphosis spinal malformation (n = 15) and controls (n = 19) were acquired from Florida Hospital. It is hypothesized that the sample of individuals with kyphosis will exhibit statistically significant covariance differences relative to the control group for T6 vertebral and midfacial linear distance measurements. Anatomical landmarks were identified on the T6 thoracic vertebrae (n = 6) and the midfacial skeleton (n = 6), and XYZ coordinates were recorded for analysis. A subset of 10 individuals (5 kyphosis, 5 controls) individuals were measured on two occasions to assess reliability and measurement error. An Euclidean Distance Matrix Analysis (EDMA) of morphological integration was carried out on the entire sample by calculating correlation values for paired linear distance measurements (one vertebral and one midfacial) separately for the kyphosis and control samples (n = 225 for each sample). Next, EDMA calculated correlation

differences and statistically assessed significance using a non-parametric bootstrap (1,000 resamples) and confidence interval testing ($\alpha \leq 0.10$). Only 35 of the 225 (15.56%) correlation differences were statistically significant. Patterns of variation among these significant correlation differences were explored by examining sample directionality of differences, sign patterns, and strengths. The relevance of these results to clinical and anthropological pursuits are discussed. Several recommendations for future investigations are made.

Acknowledgements

First and foremost, I would like to thank my committee chair, Dr. John Starbuck, for his crucial support and guidance, from the very beginning of coming up with a thesis topic all the way to completing the final draft of this thesis. I am also thankful to committee members Drs. Toyne and Williams for their guidance along the way.

I would also like to thank another committee member, Dr. William Sensakovic, and his team, as well as the Florida Hospital for providing the computed tomographic images to conduct this research topic. Without these images this research would never have been completed.

And finally, I would like to thank my parents Laura and Brian Ceuninck. Without their support and love I would not be where I am today.

Table of Contents

List of Tables

List of Figures

Introduction

Biomedical anthropology is a branch of anthropology that can be described as combining the theoretical aspects, as well as methodological aspects, of both physical anthropology and medical anthropology (Johnston and Low, 1984). Focuses within the branch of physical anthropology include, but are not limited to, the study of human biology, human diet, and human development. Some of the focuses within the branch of medical anthropology include the study of societal or group medical systems, health behaviors, and medical planning. Through the combination of these two branches of anthropology, biomedical anthropology can then be described as the understanding of the sociocultural effects of biological health and disease at both the individual and societal level. Biomedical anthropologists, therefore, inherently focus on not only the biological outcomes of studies, but also how these outcomes effect individuals and societies at large. By better understanding how atypical phenotypic structures influence development and growth, biomedical anthropologists can develop informed perspectives regarding the role that developmental change plays in the production of phenotypes and health.

By studying the health of individuals or specific groups, biomedical anthropologists may be able to learn more the medical systems in place, as well as cultural factors of a society. For example, if individuals showing atypical morphology live a long life in a population at a particular time in the Earth's history, this could be an indication that the culture in question cared for said individuals or possibly even treated them preferentially. Physical stressors, malnutrition, injury, and disease can often be preserved on the inner and outer surfaces of bone or can be observed via eroded, grown, or altered bone structures (Wippert, 2017). Diseases and physical stressors identified from bones may shed light on what kind of occupations existed in a society, whether there was an abundance or shortage of food, and what day to day life was like for

individuals. Thus, there is a clear link between anthropology and the study of human biology, health, and phenotypic abnormalities.

The vertebral column is an important feature of human anatomy, for it allows a habitual orthograde posture that allows humans to use a bipedal locomotor. In evolutionary terms of human biology was incredibly important for it created a feedback loop that resulted in other evolutionary adaptations (Vaughan, 2003). A vital component of human biology, the nervous system, is housed and protected by the vertebral column. This makes atypical phenotypical variation in the vertebral column potentially dangerous to the health and wellbeing of individuals, mainly in that it has the potential to cause various neurological disorders such as epilepsy or Parkinson's Disease. The vertebral column also correlates with other anatomical structures of the human skeletal system, such as the skull, thoracic cavity, and pelvis.

While studying morphological integration of the vertebral column relative to other anatomical structures, biomedical anthropologists will not only examine biological characteristics of an individual, but also the cultural or behavior characteristics of an individual. For example, if high numbers of correlations of integration are found between kyphotic thoracic vertebrae and the midfacial region of the skull, this may indicate widespread health problems within a population such as osteoporosis or tuberculosis (Harrison, 2007 & Jain, 2010). High numbers of correlations may also indicate certain health behaviors common in a society. For example, high amounts of correlations in kyphotic samples may indicate a cultural norm of sedentary lifestyles where a natural posture is not always achieved.

Studies of morphological integration have shown that different parts of the body may exhibit covariation due to shared developmental origins and/or functional demands (Olson, 1958). Morphological integration can be defined as "the cohesion among traits that results from

interactions of the biological processes" (Klingenberg, 2008). One instance of morphological integration may be found between the vertebral column and the skull. While the vertebral column is intimately linked to the immediately surrounding anatomy of the back, the vertebral column may also covary to some degree with superior anatomical structures, such as the craniofacial skeleton, due to the intersection of the skull with the spinal column. The vertebral column and the skull are not necessarily independent of one another due to relationships that occur from body elements being contiguous, functionally related, or developmentally related due to shared genetic origins (e.g., genetic pleiotropy, genetic cascades, complex cis- and trans-regulatory genetic mechanisms). Because the skull rests atop the vertebral column, posture, and particularly atypical postures can influence skull development, growth, and morphology during life due to the biomechanics of ambulation (Lippold, et al., 2006).

Previous studies have largely focused on the effects atypical spinal morphology has on dental morphology (Huggare, 1998), rather than the midfacial anatomy. In studies concerning the relationship between atypical spinal morphology and dental morphology, researchers found that vertebral column positioning can impact an individual's dental morphology (Saccucci et al., 2011). The relationship of the vertebral column, specifically the vertebrae of the thoracic region, has not been studied in comparison to the midfacial anatomy of the human skull prior to this study. Therefore, to the best of my knowledge, this is the first study of morphological integration focusing on both the midfacial region of the skull and the thoracic region of the spinal column.

This study specifically focuses on the atypical vertebral arrangement of kyphosis, and how kyphosis in the thoracic vertebrae may have an effect on the midfacial region of the skull. Kyphosis, also known as Scheuermann's Disease, is the atypical forward curvature of the thoracic region of the vertebral column. Generally, the vertebrae in a kyphotic thoracic region

show signs of wedging by at least five degrees in the anterior between three adjacent vertebral bodies (Tribus, 1998). The thoracic region of the vertebral column is located in the middle area of the vertebral column. The thoracic region is superior to the lumbar region and inferior to the cervical region of the spine. Overall, there are 12 distinct thoracic vertebrae and can be distinguished from cervical and lumbar vertebrae due to the nature of thoracic vertebrae articulating to the rib bones, forming the thoracic cavity (Benzel & Stillerman, 1994).

Covariation, another technique used in assessing morphological integration, can be described as the intraindividual variability among respective anatomical structures (Hooker, 2014). To understand variability at the intraindividual level, multiple measurement assessments are required in order to observe if there is any possible covariation between the anatomical structures of an individual. So, while morphological integration focuses on how anatomical structures are interrelated and interdependent on one another, covariation also studies variability in measurements among these structures.

For this investigation, it was hypothesized that a different pattern of morphological integration would be found between the kyphosis and control samples, indicating that kyphosis influences or alters craniofacial midfacial morphology. A morphometric analysis of morphological integration of the vertebral column and the midfacial region of the skull was carried out. Covariation between the T6 vertebra and midfacial measurements was calculated for each sample and correlation differences were statistically compared to assess patterns of morphological integration between these two regions of the body.

The T6 vertebrae of the thoracic column was chosen for this study for two reasons. First, the T6 vertebrae lies on the range (i.e. the T5 to T8 vertebrae) of the thoracic region where the spine naturally curves posteriorly. The second reason the T6 thoracic vertebrae was chosen is

due to certain limitations of using Amira software (v6) to visualize computed tomography images in this study. For certain individuals, some thoracic vertebrae of this range of the posterior curve would not load correctly, or there would be portions of vertebrae missing. However, the T6 thoracic vertebrae was consistent across all individuals and between samples, which is why it was specifically picked for landmark placement.

Materials and Methods

A cross-sectional sample of completely anonymized three dimensional (3D) computed tomography (CT) images of individuals with kyphosis (n = 15) and normal controls (n = 19) was acquired from Florida Hospital archives (IRBNet ID# 114278). For each individual, a CT image of the skull and spine taken within 30 days of each other were included for analysis. To control for differences in maturity, growth, and allometry, only adult individuals were included in this study. The ages and sexes of these individuals are included in Table 1. Due to the nature of the small number of individuals in both respective samples, no attempt was made to control for ethnic or ancestral backgrounds, or to divide individuals accordingly. However, in future studies that have a much larger sample size, it will be beneficial to divide individuals according to different ethnic and ancestral backgrounds to account for variation among different human populations.

Table 1: Age and Sex of Individuals Observed

Sample	Image Modality	Total n	Male n	Female n	Age Range (years)	Mean Age (years)	Standard Deviation (years)
Kyphosis	CT	15	7	8	24-71	43.24	14.06
Controls	CT	19	9	10	23-88	47.53	18.82

CT images were visualized as two-dimensional (2D) orthoslices and three-dimensional (3D) volume renderings using Amira software (v6). The orthslice for each individual was 5-millimeters in width, with 2.5-millimeter distance between slices. Six anatomical landmarks were located on the T6 thoracic vertebrae of each individual (Figure 1). An additional six anatomical landmarks were located on the midfacial region of the skull of each individual (Figure 2). Anatomical landmarks are defined in Tables 2 and 3. For a total of 10 individuals (5 kyphosis, 5 controls), anatomical landmarks were identified, and their coordinates recorded on two separate occasions with ≥24 hours in between measurements to avoid memory bias landmark placement. Coordinate values for trial 1 and trial 2 were then compared to assess measurement error and reliability by calculating mean absolute measurement error, the coefficient of reliability, and the Pearson correlation between measurements for trial 1 and 2. Following the assessment of measurement error and reliability, all other individuals were measured a single time and their coordinates were recorded for analysis. For those individuals measured twice during the measurement error and reliability analysis, their anatomical landmark coordinate values were averaged and used in further analysis.

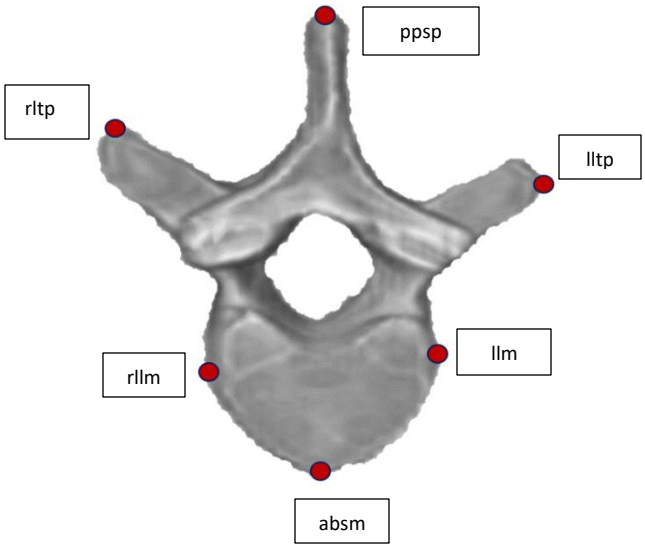

Figure 1: Anatomical landmarks located on the superior aspect of the T6 thoracic vertebrae of each individual.

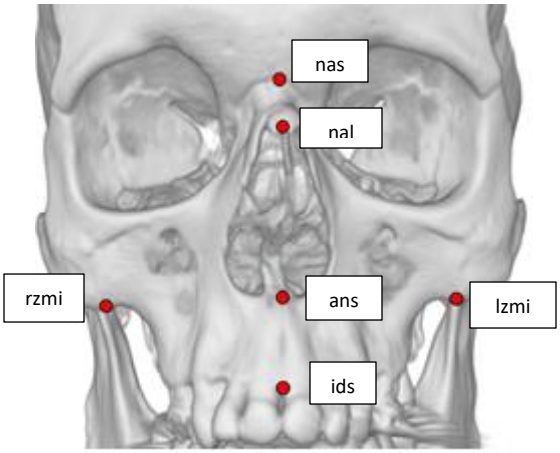

Figure 2: Anatomical landmarks located on the midfacial craniofacial skeleton of each individual.

Table 2: Anatomical landmarks and definitions measured on T6 thoracic vertebrae.

Landmark Abbreviation	Definition
1. ppsp	Posterior-most point of spinous process
2. lltp	Left lateral most point of the transverse process
3. rltp	Right lateral most point of the transverse process
4. lllm	Left lateral most point on the border of the lateral margin
5. rllm	Right lateral most point on the border of the lateral margin
6. absm	Anterior most point on the border of the super margin

Table 3: Anatomical landmarks and definitions measured on the midfacial skeleton.

Landmark Abbreviation	Definition
1. nas	Nasion – superior intersection of nasals along the midline
2. nal	Nasale – inferior point between nasals
3. ans	Anterior nasal spine – the anterior most pointed projection of the intermaxillary suture
4. ids	Intradentale Superior – point located between the superior central incisors on the alveolar maxillary border
5. lzmi	Left zygomaxillare inferior – taken on notch, most inferior point of the zygomaxillary suture in anterior view
6. rzimi	Right zygomaxillare inferior – taken on notch, most inferior point of the zygomaxillary suture in anterior view

Individual landmarks are placed on the 2-D orthoslice (Figure 3). However, it is important that each individual observed is capable of loading both an orthslice and a 3-D volume rendering. While the landmarks are actually placed on the orthslice, it is necessary to have the 3-D rendering to guide the orthoslice up and down the 3-D depiction of the anatomical structure (Figure 4). This is necessary to ensure that while placing the landmarks, the landmarks are placed in the correct anatomical region of the structure being landmarked. It is important to note that while the landmark is actually placed on a 2-D image, each landmark has its own set of X, Y, and Z coordinates. This is due to the CT image existing within a 3-D plane.

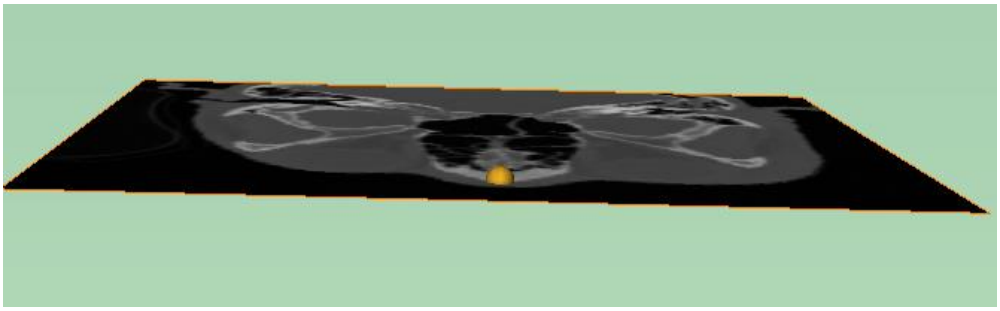

Figure 3: An example of a landmark being placed upon an 2-D orthoslice.

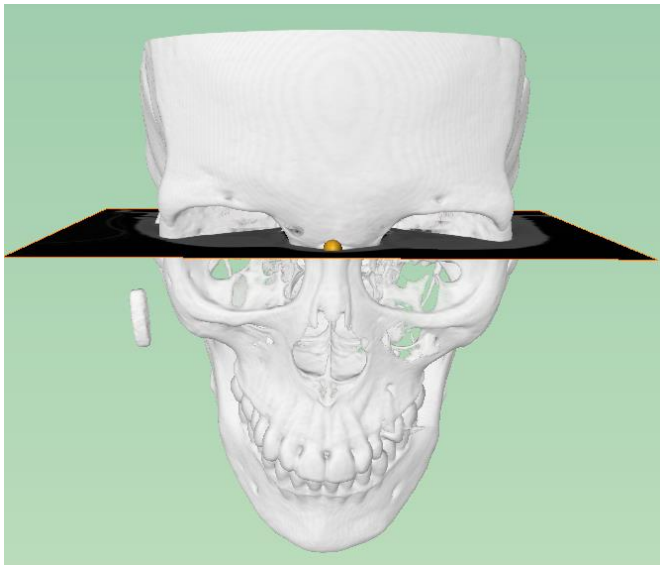

Figure 4: An example of using the 3-D volume rendering to help determine where the orthoslice is located in the 3-D plane.

Euclidean Distance Matrix Analysis

A Euclidean Distance Matrix Analysis (EDMA) approach was used to assess patterns of morphological integration between the kyphosis and control samples (Cole and Lele, 2002; Richtsmeier et al., 2006; Richtsmeier and DeLeon, 2009; Starbuck et al. 2011). Anatomical landmark coordinate XYZ files are created using a specific format and loaded into WinEDMA software (v 1.0.1). Using the utility and convert options, the XYZ file is converted into a new file consisting of all unique inter-landmark linear distances for both the midfacial region and the T6 thoracic vertebrae. EDMA software applies a formula derived from the Pythagorean theorem to calculate linear distances from XYZ coordinate values. Each individual landmark has it's own respective set of XYZ coordinate values because, while the landmark is placed on a 2-D orthographic image, the landmark still exists within a 3-D plane. Using this formula, the linear distance between any two three-dimensional (3D) anatomical landmark coordinates with

coordinate values of, for example, A = x_1,y_1,z_1 and B = x_2,y_2,z_2 can be calculated using the following formula:

$$d_{(A,B)} = \sqrt{(x_1 - x_{2)}{}^2 + (y_1 - y_2)^2 + (z_1 - z_2)^2}$$

In this equation, *d* is equal to the distance between two landmark coordinates. It is important to note that this equation can only find the distance between two points on the T6 vertebrae, or the distance between two points on the midfacial region of the skull. It cannot find the distance between one point on the vertebrae and one point on the midfacial region of the skull. The number of unique linear distances for each structure can be calculated using the following formula:

$$\frac{n(n-1)}{2},$$

where n is the number of landmarks measured.

WinEDMA software produced 4 sets of linear distance measurements (Tables 4, 5, 6, and 7), each with unique linear distances (calculated from 6 landmarks): Kyphosis vertebra, kyphosis skull, control vertebra, and control skull. Columns of measurements are defined by the two landmarks that served as the endpoints for a particular linear distance. Next, linear distance files were modified into a new format for input into the EDMA-based MIBoot program (v1.0). To accomplish this, the kyphosis linear distances for the vertebrae and skull were merged into a single file text file including 30 linear distance measurements. The same was done for the control sample. MIBoot then computed Pearson correlation matrices for each sample by calculating the pair-wise correlations between all linear distance measurements, resulting in a triangular

correlation matrix containing 435 unique correlation values for each sample (a full square matrix would contain 900 values, but 435 of them are redundant while the 30 along the diagonal are represent the correlation between a measurement and itself, or 1's and are therefore uninformative). A correlation difference matrix was automatically calculated by MIBoot by subtracting the elements of one matrix from the other. If pair-wise correlations between samples are the same, then the correlation difference matrix consists of zeros. If they are not similar, MIBoot statistically evaluates correlation differences using a non-parametric bootstrap approach (1,000 resamples) and confidence interval testing ($\alpha \leq 0.10$). The null hypothesis is that there is no difference between corresponding pair-wise correlations between the kyphosis and control samples. If a confidence interval includes the value of zero, then we fail to reject the null hypothesis. If a confidence interval does not include zero, then there is a statistically significant correlation difference between the paired linear distances in the kyphosis and control samples. Using this method, magnitude, sign relationship, and strength relationship patterns were observed to test the morphological integration of the vertebrae and midfacial region between the kyphosis and control samples. Readers are invited to review Lele and Richtsmeier (2001) for additional details about EDMA-based statistical procedures and Richtsmeier et al., 2006, Richtsmeier and DeLeon 2009, and Starbuck et al. 2011 for specific applications of MIBoot to different samples.

Table 4: Linear distance measurements from T6 vertebrae of individuals with kyphosis (n=15). Each column of measurements is defined by the two landmarks that act as endpoints for that particular linear distance measure.

	lltp& ppsp	rltp& ppsp	rltp& lltp	llm& ppsp	llm& lltp	llm& rltp	rllm& ppsp	rllm& lltp	rllm& rltp	rllm& llm	absm& ppsp	absm& lltp	absm& rltp	absm& llm	absm& rllm
K1	27.8	26.9	50.6	39.4	31.6	47.5	40.0	48.6	31.9	25.7	59.6	58.2	56.5	26.8	24.6
K2	32.9	33.9	56.6	42.7	29.6	50.1	41.9	47.9	32.1	25.8	56.6	51.6	52.7	22.4	20.6
K3	31.9	37.2	57.9	53.3	37.8	56.3	53.4	55.7	37.2	30.2	66.4	58.3	59.2	22.2	23.0
K4	29.3	26.2	52.1	49.5	43.5	55.4	48.1	58.1	40.4	28.3	61.2	61.3	60.2	19.0	22.0
K5	32.8	31.0	57.3	47.5	35.9	53.3	44.3	51.0	35.3	25.8	57.2	54.0	53.3	19.7	18.2
K6	30.4	26.1	49.8	45.9	35.1	50.9	43.7	49.8	35.2	26.2	57.3	53.5	54.5	19.3	20.2
K7	28.0	30.8	48.9	52.5	41.8	54.8	53.5	55.5	41.3	26.9	64.8	59.6	58.9	19.4	19.3
K8	33.9	30.5	57.9	48.8	37.0	54.3	47.0	53.3	37.3	26.2	60.0	55.5	56.2	19.3	19.4
K9	36.2	38.8	58.4	57.0	40.3	58.3	56.5	57.0	39.1	29.9	71.6	62.7	61.1	23.8	22.5
K10	34.3	31.5	58.6	53.7	39.7	58.7	53.9	57.0	43.4	27.7	66.7	59.4	62.9	20.4	20.7
K11	27.3	29.3	48.9	47.5	37.1	52.4	49.6	53.5	38.4	28.2	67.7	62.9	63.1	26.3	25.5
K12	39.9	39.3	61.9	58.0	38.7	59.7	59.2	58.9	42.0	30.6	69.1	56.9	61.5	19.0	21.8
K13	38.1	37.7	66.5	50.0	43.5	62.7	50.1	62.5	44.4	29.9	63.6	65.9	65.4	23.2	21.6
K14	32.1	26.1	50.1	50.0	37.2	52.2	50.5	54.6	39.1	28.0	65.5	59.9	59.3	23.5	21.4
K15	36.5	34.5	57.8	49.7	37.6	55.1	50.1	57.6	36.9	31.0	64.2	61.2	58.8	24.5	22.8

Table 5: Linear distance measurements from the midfacial region of individuals with kyphosis (n=15). Each column of measurements is defined by the two landmarks that act as endpoints for that particular linear distance measure.

	nal& nas	ans& nas	ans& nal	ids& nas	ids& nal	ids& ans	lzmi& nas	lzmi& nal	lzmi& ans	lzmi& ids	rzmi& nas	rzmi& nal	rzmi& ans	rzmi& ids	rzmi& lzmi
K1	19.3	49.8	33.1	62.0	44.4	12.9	62.0	56.5	47.2	53.6	63.6	57.8	49.5	54.9	81.0
K2	27.3	52.7	28.1	63.6	38.3	11.0	67.9	59.7	53.3	57.6	65.7	56.0	49.7	53.0	90.4
K3	21.0	52.5	34.7	72.7	54.4	20.3	73.6	67.0	54.7	59.8	72.0	64.1	51.2	56.2	93.0
K4	17.4	52.4	37.6	59.9	46.2	10.3	74.1	70.6	60.4	60.8	66.7	62.0	54.5	51.2	96.4
K5	29.7	56.1	30.9	75.3	49.4	19.2	69.9	61.3	50.6	56.6	74.8	65.3	54.2	58.6	88.2
K6	22.1	54.6	36.4	68.1	49.5	13.5	67.3	63.7	55.4	60.2	68.2	63.4	55.2	60.1	89.8
K7	16.2	46.9	34.4	67.3	54.3	20.5	67.6	64.2	49.1	52.5	67.8	61.4	46.4	51.4	83.0
K8	24.1	54.7	32.9	66.8	45.1	12.3	64.6	56.1	47.8	50.6	66.1	58.1	51.7	55.3	82.7
K9	17.6	54.5	38.0	67.7	51.3	13.3	69.7	62.6	52.3	55.2	70.3	62.4	52.8	55.8	88.4
K10	22.2	50.1	30.2	64.7	44.8	14.7	68.3	60.5	52.5	54.9	71.4	62.6	50.8	52.1	89.0
K11	19.0	54.3	37.3	71.3	53.6	17.4	77.9	70.2	55.9	61.1	76.5	69.1	58.3	63.1	101.2
K12	24.6	53.3	34.1	72.5	53.6	19.7	73.2	70.4	58.2	60.9	76.3	71.9	59.9	62.5	93.6
K13	18.9	52.1	37.2	70.7	54.8	18.7	70.6	64.9	49.5	54.8	72.5	65.1	49.2	53.3	88.0
K14	18.0	55.2	38.0	78.0	60.8	22.8	74.0	66.1	56.0	61.5	76.6	67.5	55.7	61.2	97.7
K15	21.7	52.3	34.0	64.1	46.2	12.2	63.9	57.1	46.4	47.0	63.7	56.5	46.8	49.7	79.5

Table 6: Linear distance measurements from T6 vertebrae of individuals in the control sample (n=17). Each column of measurements is defined by the two landmarks that act as endpoints for that particular linear distance measure.

	ltp& ppsp	rltp& ppsp	rltp& lltp	lllm& ppsp	lllm& lltp	lllm& rltp	rllm& ppsp	rllm& lltp	rllm& rltp	rllm& lllm	absm& ppsp	absm& lltp	absm& rltp	absm& lllm	absm& rllm
C1	28.1	28.4	50.9	40.2	29.5	47.4	40.4	47.2	30.0	26.6	50.4	47.2	47.2	18.7	18.1
C2	35.6	31.4	60.1	56.3	41.5	60.6	58.2	63.6	43.9	33.9	74.5	67.9	67.4	27.4	25.3
C3	40.4	34.3	60.3	55.7	41.4	59.8	52.4	59.1	40.1	31.1	73.6	67.6	68.6	26.6	29.0
C4	24.0	53.0	32.8	66.8	46.8	14.1	66.4	59.9	51.6	53.6	63.1	57.4	47.3	51.4	79.5
C5	34.3	37.2	59.3	52.4	36.5	60.5	50.4	52.5	40.3	29.2	65.1	57.6	61.7	22.7	21.6
C6	28.0	28.8	49.3	45.0	35.5	51.9	45.9	51.2	37.5	26.8	58.2	56.1	55.2	22.2	18.4
C7	31.9	34.0	58.5	50.8	39.7	57.5	53.9	58.4	43.1	28.3	65.6	60.8	62.0	21.8	20.1
C8	30.3	36.9	64.2	45.9	41.3	57.3	49.4	60.4	40.0	28.3	60.8	62.4	59.5	21.6	20.1
C9	28.6	29.9	52.8	47.1	34.9	53.2	47.6	51.1	37.4	26.8	65.5	58.8	61.6	24.2	24.7
C10	30.7	33.9	53.6	45.3	35.1	51.9	47.1	53.0	35.1	28.4	60.4	57.8	56.7	23.5	22.3
C11	26.4	25.6	46.4	46.4	35.9	50.1	48.2	52.4	37.0	28.1	61.8	57.2	57.1	22.2	22.0
C12	30.7	31.4	53.0	53.6	39.8	54.8	57.2	59.0	41.4	30.2	66.8	59.6	58.7	21.0	20.1
C13	34.8	33.0	56.4	52.2	40.6	56.4	52.5	57.8	40.6	28.5	64.6	60.7	59.4	21.3	20.0
C14	32.6	32.4	51.5	55.7	40.0	55.7	56.2	56.7	40.2	30.1	67.4	58.5	59.0	20.1	21.4
C15	35.5	34.9	61.5	52.1	39.6	58.3	53.2	59.8	40.3	30.7	71.7	66.3	65.7	27.0	26.0
C16	26.2	31.4	54.4	41.5	34.0	51.5	43.0	49.4	36.4	24.0	62.7	60.2	60.9	26.2	24.4
C17	33.3	34.2	53.4	55.3	38.2	57.7	56.3	57.0	40.3	32.8	69.3	60.3	61.4	24.0	23.1
C18	19.4	51.5	33.3	71.7	53.8	20.5	70.7	63.8	55.5	59.2	73.1	66.0	56.6	58.8	86.8
C19	40.8	38.4	58.4	59.3	38.7	58.9	59.3	59.5	39.8	33.7	71.9	61.0	60.5	24.0	22.5

Table 7: Linear distance measurements from midfacial region of individuals in the control sample (c=19). Each column of measurements is defined by the two landmarks that act as endpoints for that particular linear distance measure.

	nal& nas	ans& nas	ans& nal	ids& nas	ids& nal	ids& ans	lzmi& nas	lzmi& nal	lzmi& ans	lzmi& ids	rzmi& nas	rzmi& nal	rzmi& ans	rzmi& ids	rzmi& lzmi
C1	21.0	52.6	36.9	70.1	54.5	17.7	65.8	63.0	52.0	56.4	64.2	60.6	49.4	54.3	82.4
C2	25.1	58.6	36.5	76.3	54.0	17.8	73.3	64.1	51.8	57.4	76.0	66.2	54.1	56.4	90.2
C3	25.2	58.8	40.3	73.7	54.3	14.9	72.1	66.4	49.9	54.1	73.8	67.9	52.0	56.5	85.5
C4	24.0	53.0	32.8	66.8	46.8	14.1	66.4	59.9	51.6	53.6	63.1	57.4	47.3	51.4	79.5
C5	21.1	52.6	32.1	75.2	54.3	22.9	72.1	61.4	49.6	57.5	70.5	58.1	48.5	55.5	87.2
C6	21.0	50.5	32.3	68.0	49.1	17.7	68.6	62.6	53.0	58.6	69.0	61.1	49.9	55.0	88.6
C7	18.3	53.7	37.6	68.5	51.8	14.9	67.6	60.7	48.5	54.0	69.2	60.6	48.5	52.5	86.5
C8	29.8	54.8	30.6	70.8	44.7	16.5	69.1	59.3	47.1	53.9	72.5	63.5	54.7	59.3	92.0
C9	21.5	51.0	33.5	70.8	52.5	19.8	67.4	60.9	51.1	57.2	68.1	61.1	49.6	55.5	91.5
C10	16.4	50.6	35.8	60.8	46.4	10.7	65.5	60.1	50.4	50.8	64.5	57.7	47.2	48.5	82.0
C11	17.7	44.5	30.0	65.3	49.6	21.2	65.8	60.6	47.6	53.9	65.0	59.0	46.5	53.1	79.6
C12	21.6	50.5	32.0	63.2	45.0	13.0	62.3	57.4	48.5	51.5	63.2	56.1	48.7	51.1	81.3
C13	26.0	56.3	38.0	66.7	48.6	10.7	75.5	70.9	55.3	56.7	76.6	72.3	56.5	56.0	95.1
C14	24.4	55.5	33.6	74.8	51.7	19.9	74.6	66.0	56.1	63.5	79.6	70.7	61.7	68.5	104.6
C15	15.4	59.8	47.2	71.8	59.3	12.1	76.3	70.0	49.8	50.3	73.4	68.4	49.0	51.1	79.8
C16	18.6	50.3	33.0	65.9	48.3	15.6	67.4	58.2	44.6	48.1	67.0	57.0	44.8	47.8	76.5
C17	14.3	47.3	34.3	66.0	53.2	19.0	68.7	64.5	55.4	57.5	66.9	62.4	53.4	57.3	86.5
C18	17.7	49.0	33.4	59.5	45.4	13.7	68.6	60.9	48.2	44.1	69.8	63.9	49.4	45.0	76.8
C19	13.6	52.4	40.1	72.1	59.8	19.7	77.8	73.3	59.5	62.4	74.2	68.2	54.8	59.6	94.9

The hypothesis tested in this project was formulated to assess the relationship between the midfacial region of the skull and the T6 thoracic vertebra. Consequently, all correlations within structures (e.g. skull measure correlated to skull measure, or vertebral measure correlated to vertebral measure) that were automatically calculated by MIBoot software were removed from the analysis. This resulted in two 15 X 15 correlation matrices (kyphosis and control) (Table 8 and 9) and one 15 X 15 correlation difference matrix (Table 10). Each of these matrices contained 225 correlation or correlation difference values of potential interest with respect to the hypothesis tested here. Accordingly, it is these 225 correlation difference values that were statistically assessed and reported here. Once statistical significant differences in correlation values were ascertained, patterns in original correlation values between samples were explored.

Table 8: Kyphosis sample correlations between vertebrae and skull measures. Linear distances are defined by the two anatomical landmark endpoints listed for each column or row.

	lltp& ppsp	rltp& ppsp	rltp& lltp	lllm& ppsp	lllm& lltp	lllm& rltp	rllm& ppsp	rllm& lltp	rllm& rltp	rllm& lllm	absm& ppsp	absm& lltp	absm& rltp	absm& lllm	absm& rllm
nal&nas	0.32	0.17	0.36	-0.20	-0.55	-0.15	-0.32	-0.42	-0.41	-0.32	-0.50	-0.75	-0.60	-0.32	-0.46
ans&nas	0.26	0.00	0.13	0.01	-0.20	-0.07	-0.11	-0.15	-0.22	0.02	-0.10	-0.22	-0.22	-0.03	-0.08
ans&nal	-0.08	-0.09	-0.20	0.29	0.56	0.24	0.33	0.46	0.38	0.46	0.46	0.67	0.53	0.20	0.39
ids&nas	0.21	0.18	0.11	0.32	0.06	0.17	0.31	0.11	0.19	0.17	0.26	0.01	0.10	-0.02	-0.15
ids&nal	0.06	0.11	-0.07	0.49	0.48	0.34	0.54	0.45	0.50	0.43	0.55	0.47	0.49	0.06	0.11
ids&ans	0.06	0.17	0.02	0.38	0.24	0.25	0.44	0.26	0.38	0.22	0.37	0.18	0.29	-0.03	-0.10
lzmi&nas	-0.05	0.08	-0.05	0.40	0.37	0.29	0.43	0.34	0.42	0.36	0.45	0.32	0.47	-0.03	0.26
lzmi&nal	-0.07	0.07	-0.11	0.44	0.49	0.33	0.48	0.42	0.49	0.41	0.43	0.33	0.49	-0.18	0.25
lzmi&ans	-0.08	-0.11	-0.18	0.29	0.18	0.09	0.27	0.13	0.22	0.18	0.21	-0.03	0.19	-0.29	0.14
lzmi&ids	-0.21	-0.18	-0.25	0.08	-0.02	-0.07	0.09	-0.08	0.06	-0.01	0.10	-0.11	0.08	-0.13	0.17
rzmi&nas	0.20	0.19	0.14	0.46	0.25	0.36	0.48	0.29	0.45	0.27	0.47	0.20	0.42	-0.04	0.02
rzmi&nal	0.17	0.15	0.07	0.50	0.35	0.38	0.53	0.37	0.51	0.34	0.50	0.24	0.49	-0.13	0.12
rzmi&ans	0.04	-0.11	-0.12	0.22	0.00	0.01	0.20	-0.01	0.10	0.08	0.22	-0.10	0.12	-0.15	0.16
rzmi&ids	-0.03	-0.08	-0.19	0.08	-0.23	-0.16	0.10	-0.21	-0.07	-0.03	0.18	-0.17	0.00	0.06	0.16
rzmi&lzmi	-0.16	-0.12	-0.20	0.19	0.14	0.06	0.22	0.11	0.23	0.16	0.28	0.13	0.30	0.00	0.28

Table 9: Control sample correlations between vertebrae and skull measures. Linear distances are defined by the two anatomical landmark endpoints listed for each column or row.

	lltp& ppsp	rltp& ppsp	rltp& lltp	lllm& ppsp	lllm& lltp	lllm& rltp	rllm& ppsp	rllm& lltp	rllm& rltp	rllm& lllm	absm& ppsp	absm& lltp	absm& rltp	absm& lllm	absm& rllm
nal&nas	0.02	0.00	0.13	-0.04	0.17	0.01	-0.05	0.17	0.09	-0.05	-0.13	0.08	0.00	-0.06	-0.02
ans&nas	0.58	0.06	0.51	0.11	0.16	0.29	0.08	0.42	0.07	-0.07	0.35	0.46	0.44	-0.09	-0.11
ans&nal	0.60	0.00	0.40	0.10	0.01	0.28	0.05	0.26	-0.07	-0.07	0.40	0.38	0.41	-0.08	-0.12
ids&nas	0.64	-0.24	0.57	-0.09	-0.22	0.52	-0.15	0.05	-0.21	-0.33	0.22	0.14	0.44	-0.39	-0.39
ids&nal	0.68	-0.23	0.45	-0.02	-0.30	0.47	-0.10	-0.04	-0.28	-0.25	0.32	0.10	0.41	-0.30	-0.33
ids&ans	0.10	-0.27	0.09	-0.13	-0.33	0.25	-0.18	-0.33	-0.24	-0.22	-0.06	-0.28	0.05	-0.27	-0.26
lzmi&nas	0.66	0.07	0.42	0.27	0.17	0.37	0.20	0.37	0.08	-0.02	0.53	0.45	0.50	-0.09	-0.13
lzmi&nal	0.69	-0.04	0.33	0.21	0.03	0.33	0.14	0.26	-0.07	-0.06	0.40	0.26	0.32	-0.17	-0.19
lzmi&ans	0.48	0.01	0.04	0.26	-0.04	0.16	0.22	0.11	-0.06	0.03	0.16	-0.14	-0.06	-0.17	-0.14
lzmi&ids	0.55	-0.35	0.32	-0.11	-0.36	0.46	-0.14	-0.15	-0.34	-0.37	-0.05	-0.28	0.05	-0.54	-0.49
rzmi&nas	0.58	-0.04	0.46	0.21	0.24	0.43	0.17	0.43	0.11	-0.09	0.52	0.52	0.58	-0.17	-0.19
rzmi&nal	0.55	-0.01	0.32	0.27	0.26	0.30	0.23	0.44	0.09	0.01	0.48	0.45	0.42	-0.09	-0.10
rzmi&ans	0.48	-0.05	0.29	0.22	0.18	0.33	0.23	0.38	0.04	-0.06	0.30	0.21	0.24	-0.24	-0.21
rzmi&ids	0.54	-0.29	0.39	-0.05	-0.18	0.48	-0.07	0.04	-0.25	-0.33	0.07	-0.07	0.19	-0.50	-0.45
rzmi&lzmi	0.51	-0.23	0.40	-0.01	-0.09	0.47	-0.01	0.11	-0.16	-0.30	0.12	0.01	0.23	-0.45	-0.42

Table 10: Correlation difference matrix for kyphosis and control samples. Linear distances are defined by the two anatomical landmarks listed for each column or row.

	lltp& ppsp	rltp& ppsp	rltp& lltp	lllm& ppsp	lllm& lltp	lllm& rltp	rllm& ppsp	rllm& lltp	rllm& rltp	rllm& lllm	absm& ppsp	absm& lltp	absm& rltp	absm& lllm	absm& rllm
nal&nas	0.30	0.17	0.22	-0.15	-0.71	-0.16	-0.27	-0.59	-0.50	-0.27	-0.37	-0.83	-0.59	-0.26	-0.45
ans&nas	-0.32	-0.06	-0.38	-0.10	-0.36	-0.36	-0.19	-0.56	-0.29	0.09	-0.45	-0.68	-0.67	0.07	0.03
ans&nal	-0.68	-0.09	-0.61	0.20	0.56	-0.04	0.28	0.20	0.45	0.52	0.06	0.29	0.12	0.28	0.51
ids&nas	-0.43	0.41	-0.47	0.41	0.27	-0.35	0.46	0.06	0.40	0.50	0.05	-0.14	-0.33	0.37	0.24
ids&nal	-0.62	0.33	-0.52	0.51	0.79	-0.13	0.64	0.49	0.79	0.68	0.23	0.37	0.08	0.36	0.44
ids&ans	-0.03	0.44	-0.07	0.51	0.58	0.00	0.62	0.59	0.62	0.44	0.43	0.46	0.24	0.24	0.16
lzmi&nas	-0.72	0.01	-0.48	0.13	0.20	-0.08	0.23	-0.02	0.33	0.38	-0.08	-0.13	-0.03	0.07	0.39
lzmi&nal	-0.76	0.10	-0.43	0.22	0.45	0.00	0.33	0.16	0.56	0.46	0.03	0.07	0.18	-0.01	0.43
lzmi&ans	-0.56	-0.12	-0.22	0.03	0.22	-0.06	0.05	0.02	0.28	0.15	0.05	0.10	0.25	-0.13	0.28
lzmi&ids	-0.75	0.17	-0.56	0.19	0.34	-0.53	0.23	0.06	0.40	0.36	0.15	0.17	0.04	0.41	0.66
rzmi&nas	-0.37	0.24	-0.32	0.25	0.02	-0.07	0.31	-0.13	0.35	0.36	-0.05	-0.33	-0.16	0.12	0.22
rzmi&nal	-0.39	0.15	-0.25	0.23	0.09	0.09	0.30	-0.07	0.42	0.33	0.02	-0.21	0.07	-0.04	0.22
rzmi&ans	-0.44	-0.06	-0.42	0.00	-0.19	-0.32	-0.03	-0.39	0.06	0.13	-0.09	-0.30	-0.12	0.09	0.37
rzmi&ids	-0.56	0.20	-0.58	0.13	-0.05	-0.63	0.17	-0.25	0.18	0.30	0.10	-0.10	-0.18	0.56	0.61
rzmi&lzmi	-0.67	0.11	-0.60	0.20	0.22	-0.41	0.24	0.00	0.39	0.46	0.16	0.12	0.07	0.45	0.69

Results

For T6 vertebra landmarks the overall absolute measurement error was 0.14mm. The vertebral coefficient of reliability was 0.54, and the Pearson correlation was 1.00. For skull landmarks the overall absolute measurement error was 0.13mm. The skull coefficient of reliability was 0.73, and the Pearson correlation was also 1.00. Overall these results suggest that there is increased measurement error associated with vertebral landmarks relative to skull landmarks, but the absolute measurement error is fairly low for each subsample.

Statistical comparison of the correlation matrices for the kyphosis and control samples revealed that 35 out of 225 (15.56%) linear distance pairs from the skull and spine are significantly different (Tables 11 and 12; Figure 3) by confidence interval testing ($\alpha \leq 0.10$). Since this study is focusing on difference correlations to determine differences in morphological integration of the midfacial region of the skull and the T6 thoracic vertebrae, these 35 significant distances were statistically assessed and closely examined. To explore patterns of variation associated with these results, significant differences were categorized based on whether: 1) the correlation difference was higher in magnitude in one sample relative to the other, 2) the sign patterns of the correlation values between samples (positive, negative), and 3) the strength of the relationship between samples (absolute value of 0-0.1 very weak, 0.11-0.30 weak, 0.31-0.5 moderate, and 0.51-1.00 strong). Using these interpretive frameworks allowed us to identify the following patterns in the significant results.

Table 11: Correlation values for each sample, negative correlation differences, and 90% confidence intervals are shown for significant pairs of linear distance measures from the T6 vertebra and midfacial region of the skull. Negative correlation differences indicate that the control correlation is either greater than the kyphosis correlation and/or the norm correlation is positive when the kyphosis correlation is negative. All 90% confidence intervals shown do not include the value of 0 (null hypothesis) and are statistically significant. Paired linear distance correlation values from each sample are labeled based on their sign and strength relationships.

Linear Distance Pair		Kyphosis *r*	Control *r*	Difference	Lo90	Hi90	Sign Relationship (+/-)	Strength Relationship
nal&nas	**lllm&lltp**	-0.55	0.17	-0.71	-1.22	-0.30	Negative/Positive	Strong/Weak
nal&nas	**rllm&lltp**	-0.42	0.17	-0.59	-1.04	-0.07	Negative/Positive	Moderate/Weak
nal&nas	**rllm&rltp**	-0.41	0.09	-0.50	-0.99	-0.01	Negative/Positive	Moderate/Very Weak
nal&nas	**absm&lltp**	-0.75	0.08	-0.83	-1.17	-0.43	Negative/Positive	Strong/Very Weak
nal&nas	**absm&rltp**	-0.60	0.01	-0.61	-0.99	-0.04	Negative/Negative	Strong/Very Weak
ans&nas	**rllm&lltp**	-0.15	0.42	-0.56	-1.03	-0.08	Negative/Positive	Weak/Moderate
ans&nas	**absm&lltp**	-0.22	0.46	-0.68	-1.09	-0.19	Negative/Positive	Weak/Moderate
ans&nas	**absm&rltp**	-0.22	0.44	-0.67	-1.12	-0.18	Negative/Positive	Weak/Moderate
ans&nal	**lltp&ppsp**	-0.08	0.60	-0.68	-1.08	-0.33	Negative/Positive	Weak/Strong
ans&nal	**rltp&lltp**	-0.20	0.40	-0.61	-1.15	-0.17	Negative/Positive	Weak/Moderate
ids&nas	**lltp&ppsp**	0.21	0.64	-0.43	-0.84	-0.03	Negative/Positive	Weak/Strong
ids&nas	**rltp&lltp**	0.11	0.57	-0.47	-0.89	-0.01	Negative/Positive	Weak/Strong
ids&nal	**lltp&ppsp**	0.06	0.68	-0.62	-1.02	-0.20	Negative/Positive	Very Weak/Strong
lzmi&nas	**lltp&ppsp**	-0.05	0.66	-0.72	-1.26	-0.17	Negative/Positive	Very Weak/Strong
lzmi&nal	**lltp&ppsp**	-0.07	0.69	-0.76	-1.35	-0.26	Negative/Positive	Very Weak/Strong
lzmi&ids	**lltp&ppsp**	-0.21	0.55	-0.75	-1.26	-0.14	Negative/Positive	Weak/Strong
lzmi&ids	**lllm&rltp**	-0.07	0.46	-0.53	-0.98	-0.05	Negative/Positive	Very Weak/Moderate
rzmi&ids	**lllm&rltp**	-0.16	0.48	-0.63	-1.09	-0.22	Negative/Positive	Weak/Moderate
rzmi&lzmi	**lltp&ppsp**	-0.16	0.51	-0.67	-1.22	-0.10	Negative/Positive	Weak/Strong
rzmi&lzmi	**rltp&lltp**	-0.20	0.40	-0.60	-1.08	-0.05	Negative/Positive	Weak/Moderate
rzmi&lzmi	**lllm&rltp**	0.06	0.47	-0.41	-0.84	-0.01	Positive/Positive	Very Weak/Moderate

Table 12: Correlation values for each sample, positive correlation differences, and 90% confidence intervals are shown for significant pairs of linear distance measures from the vertebrae and midfacial region of the skull. Positive correlation differences indicate that the kyphosis correlation is either greater than the control correlation and/or the kyphosis correlation is positive when the control correlation is negative. All 90% confidence intervals shown do not include the value of 0 (null hypothesis) and are statistically significant. Paired linear distance correlation values from each sample are labeled based on their sign and strength relationships.

Linear Distance Pair		Kyphosis *r*	Control *r*	Difference	Lo90	Hi90	Sign Relationship (+/-) Kyphosis/Control	Strength Relationship Kyphosis/Control
rzmi&lzmi	**absm&rllm**	0.28	-0.42	0.69	0.01	1.25	Positive/Negative	Weak/Moderate
ans&nal	**lllm&lltp**	0.56	0.01	0.56	0.06	0.89	Positive/Positive	Strong/Very Weak
ans&nal	**rllm&llllm**	0.46	-0.07	0.52	0.03	0.83	Positive/Negative	Moderate/Very Weak
ids&nal	**lllm&lltp**	0.48	-0.30	0.79	0.18	1.22	Positive/Negative	Moderate/Moderate
ids&nal	**rllm&ppsp**	0.54	-0.10	0.64	0.13	1.06	Positive/Negative	Strong/Weak
ids&nal	**rllm&rltp**	0.50	-0.28	0.79	0.21	1.19	Positive/Negative	Strong/Weak
ids&ans	**lllm&ppsp**	0.06	0.10	0.51	0.06	0.91	Positive/Positive	Very Weak/Very Weak
ids&ans	**lllm&lltp**	0.24	-0.33	0.58	0.07	1.08	Positive/Negative	Weak/Moderate
ids&ans	**rllm&ppsp**	0.44	-0.18	0.62	0.18	1.02	Positive/Negative	Moderate/Weak
ids&ans	**rllm&lltp**	0.26	-0.33	0.59	0.10	1.05	Positive/Negative	Weak/Moderate
ids&ans	**rllm&rltp**	0.38	-0.24	0.62	0.19	1.04	Positive/Negative	Moderate/Weak
ids&ans	**absm&lltp**	0.18	-0.28	0.46	0.01	0.89	Positive/Negative	Weak/Weak
lzmi&nal	**rllm&rltp**	0.49	-0.07	0.56	0.15	0.88	Positive/Negative	Moderate/Very Weak
lzmi&ids	**absm&rllm**	0.17	-0.49	0.66	0.08	1.21	Positive/Negative	Weak/Moderate

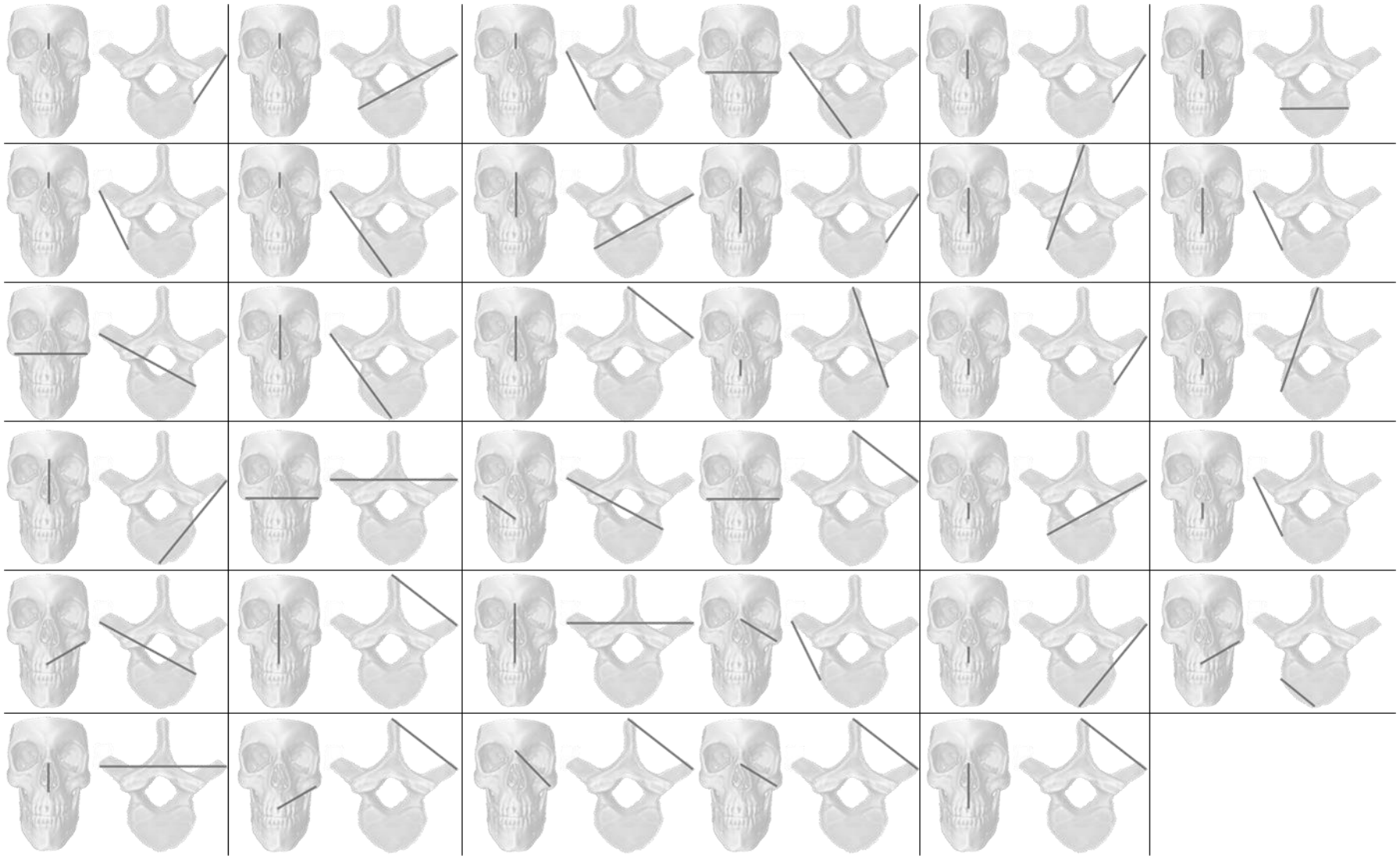

Figure 3: All paired linear distances that significantly differ between the kyphosis and control samples.

Correlation Difference Magnitude Patterns

Of the 35 significant correlation differences, the correlation values of 21 were higher in the control sample (Figure 4), while the remaining 14 were larger in the kyphosis sample (Figure 5). Often this represents a situation where a correlation is positive in the sample with a higher value, and negative or lower in the other sample (Figure 6). Thus, 60% of significant correlation differences represent a relationship where original correlation values exhibited relatively higher integration in the control sample.

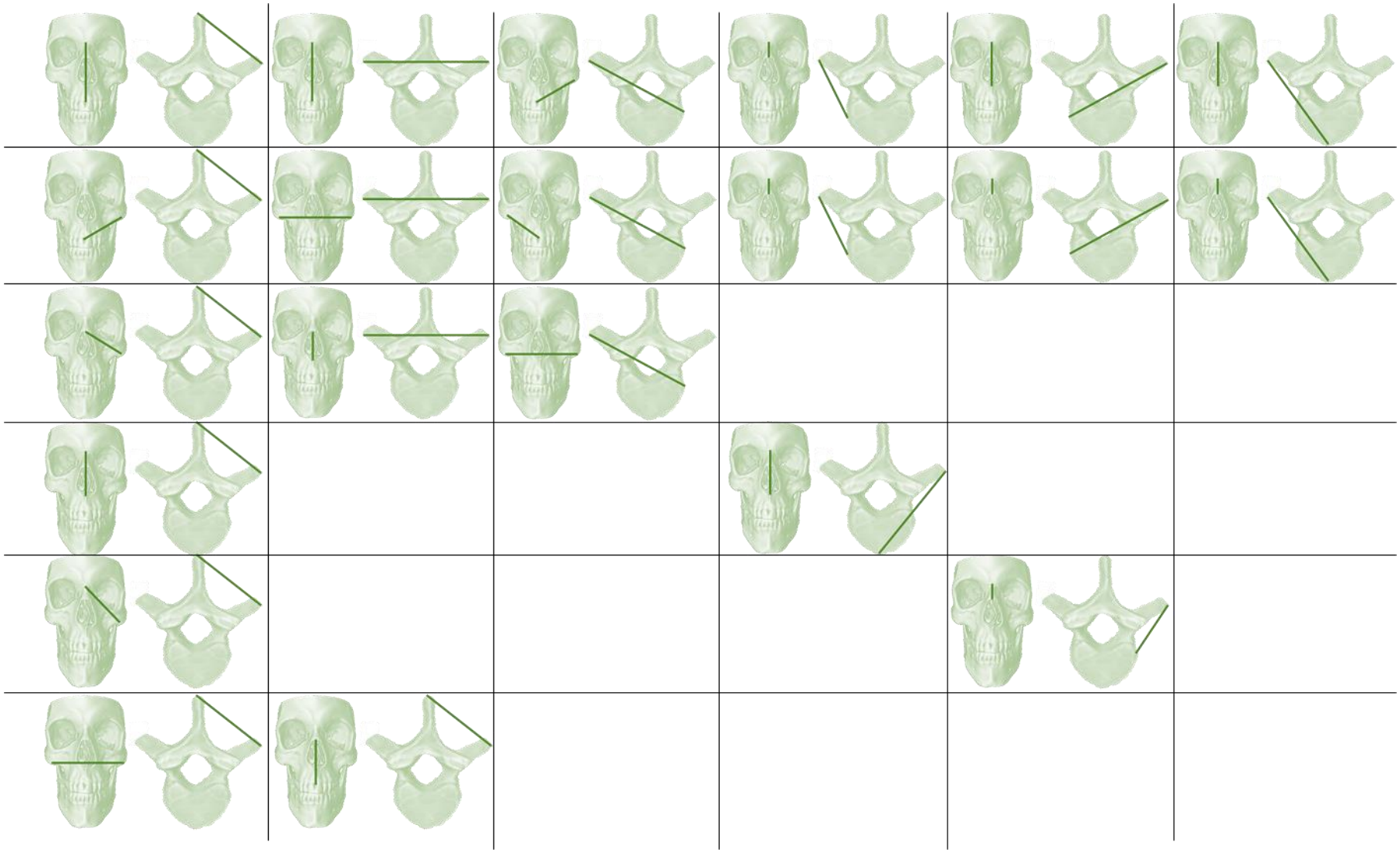

Figure 4: Significant negative correlation differences are depicted in green. Negative correlation differences indicate that the control correlation is either greater than the kyphosis correlation and/or the control correlation is positive when the kyphosis correlation is negative. Correlations involving the same linear distance measure from the vertebra are stacked or next to each other to observe patterns in the results, while others are spaced out.

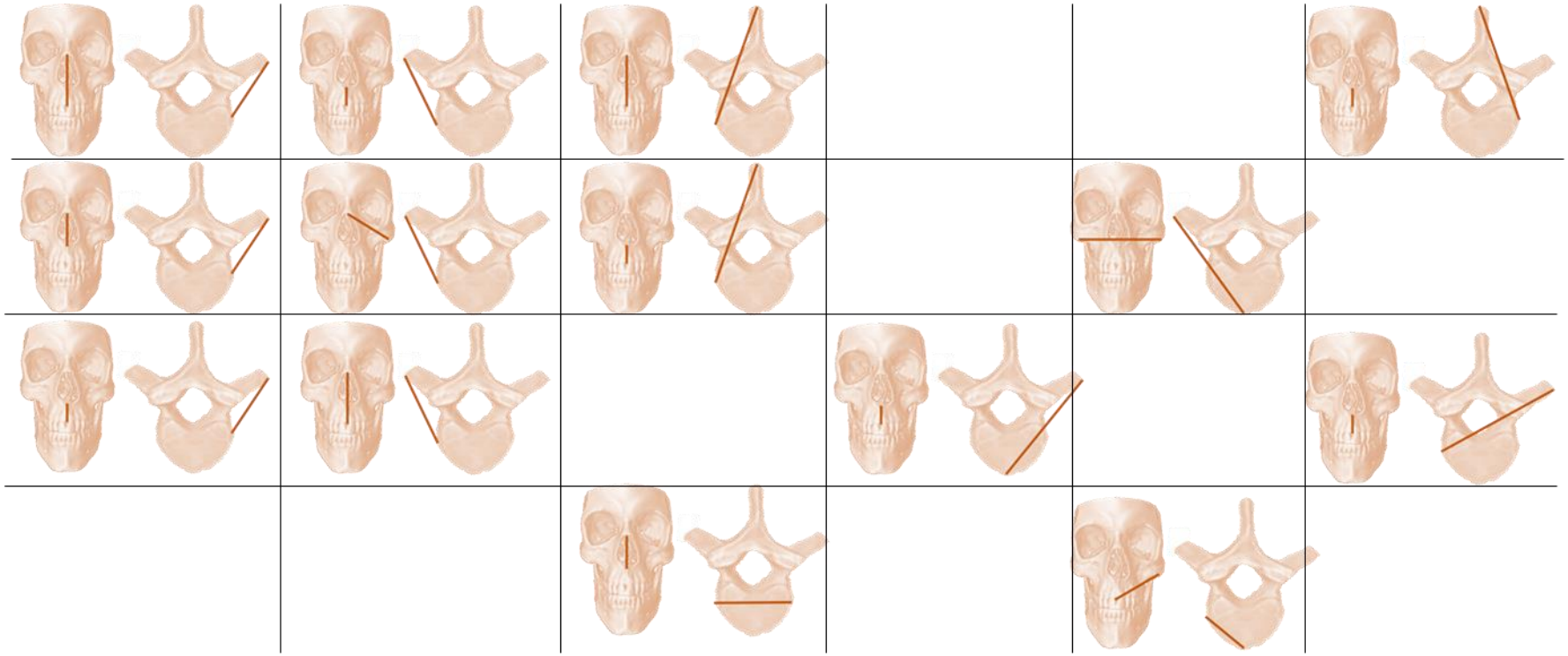

Figure 5: Significant positive correlation differences are depicted in red. Positive correlation differences indicate that the kyphosis correlation is either greater than the control correlation and/or the kyphosis correlation is positive when the control correlation is negative. Correlations involving the same linear distance measure from the vertebra are stacked to observe patterns in the results, while others are spaced out.

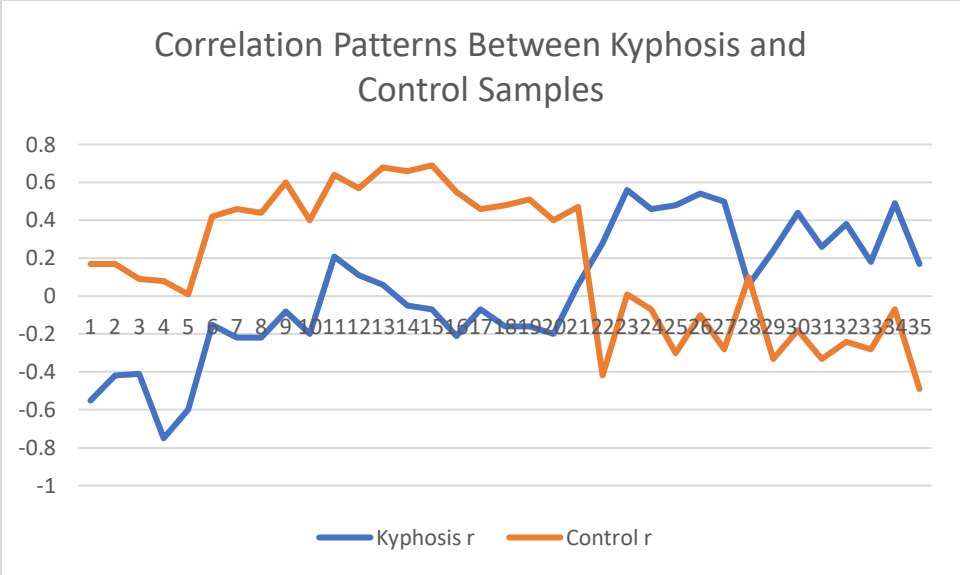

Figure 6: Patterns of significant correlation differences between samples. The magnitude of integration (i.e., space between corresponding points on this figure) was larger in the control sample for 21 of the 35 significant correlation differences, and higher for the kyphosis sample for the other 14 significant differences.

Correlation Sign Patterns

By looking at the sign of the original correlation values from each sample for each significant correlation difference, the results were divided as follows: negative/positive (n = 19), positive/negative (n = 12), positive/positive (n = 3), and negative/negative (n = 1) (Figure 7). Thus, the majority of integration patterns illustrate a relationship where values are negative in the kyphosis sample and positive in the control sample, or positive in the kyphosis sample and negative in the control sample. Very few significant results exist where the correlation signs are identical in both samples.

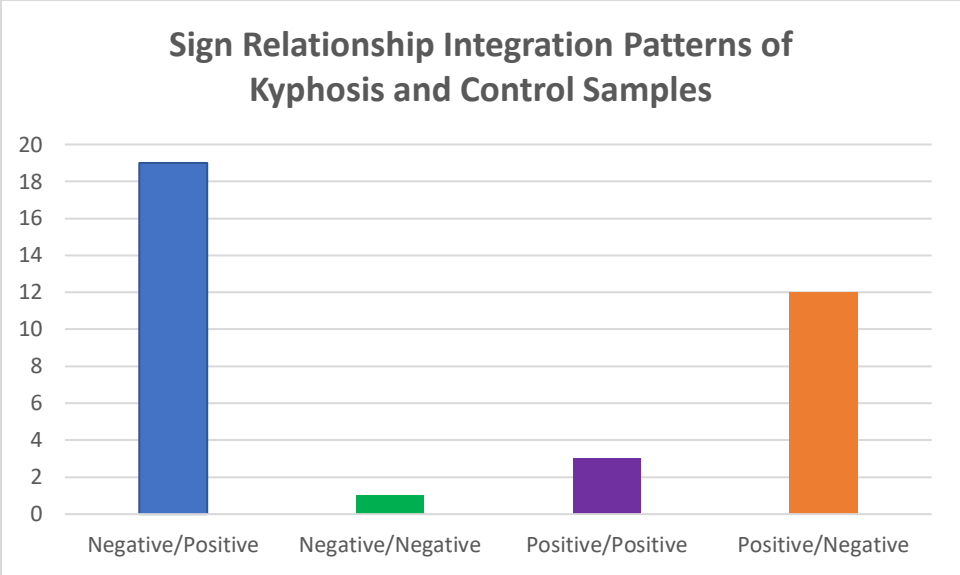

Figure 7: Bar graph summarizing the different patterns of sign relationship proportions between the kyphosis and control samples. The first sign listed is for the kyphosis sample. The second sign listed is for the control sample.

Thus, it is more likely for negative correlation values to be associated with the kyphosis sample when positive corresponding values are found in the control sample (19/35, or 54.3% of the time), but this pattern is not consistent (Figure 8, 9, 10, and 11). In many situations the correlation value is positive in the kyphosis sample and negative in the control sample (12/35, or 34.3% of the time), although this occurs less frequently.

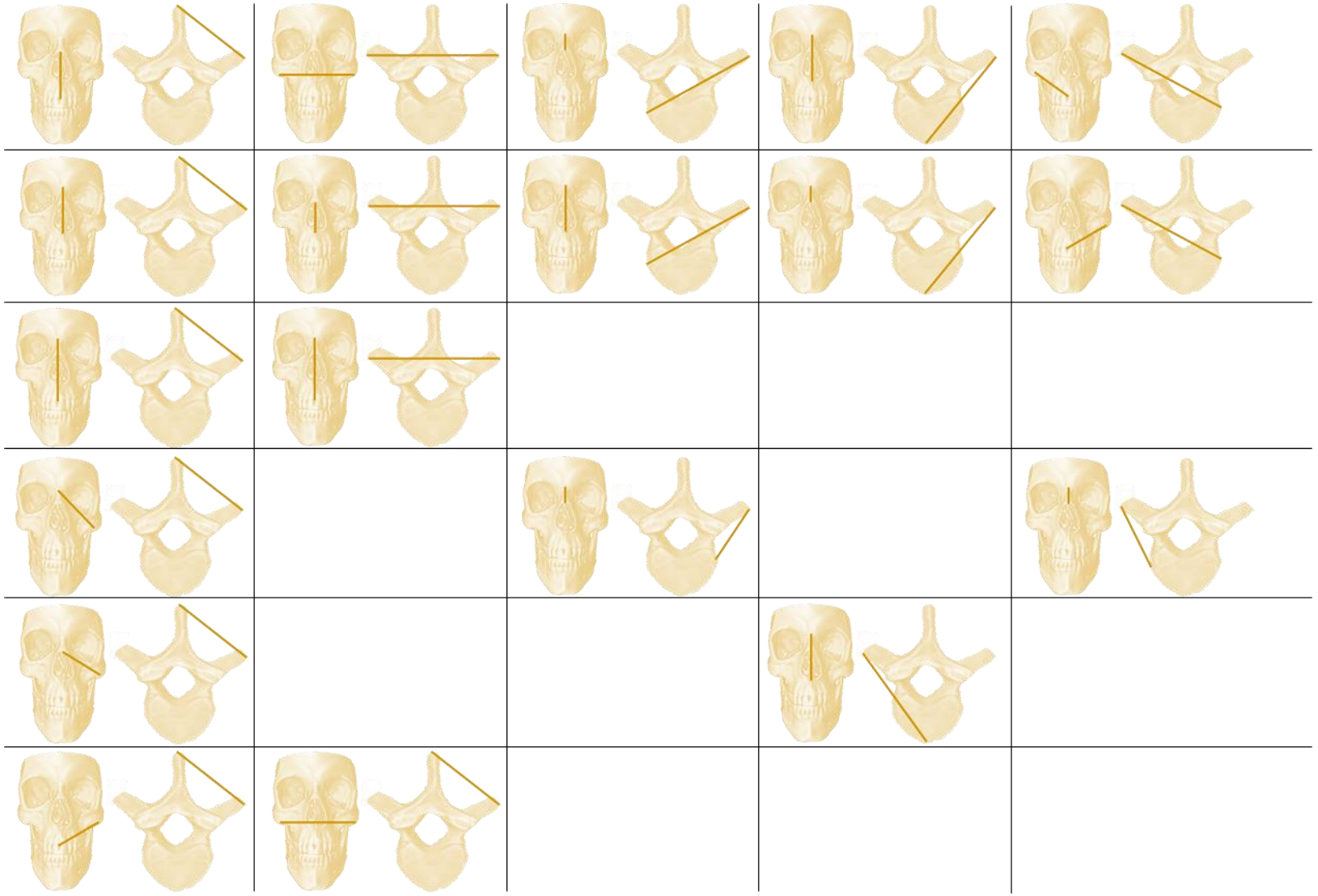

Figure 8: Significant correlation differences are depicted in orange where the original correlation was negative in the kyphosis sample and positive in the control sample. Correlations involving the same linear distance measure from the vertebra are stacked or next to each other to observe patterns in the results, while others are spaced out.

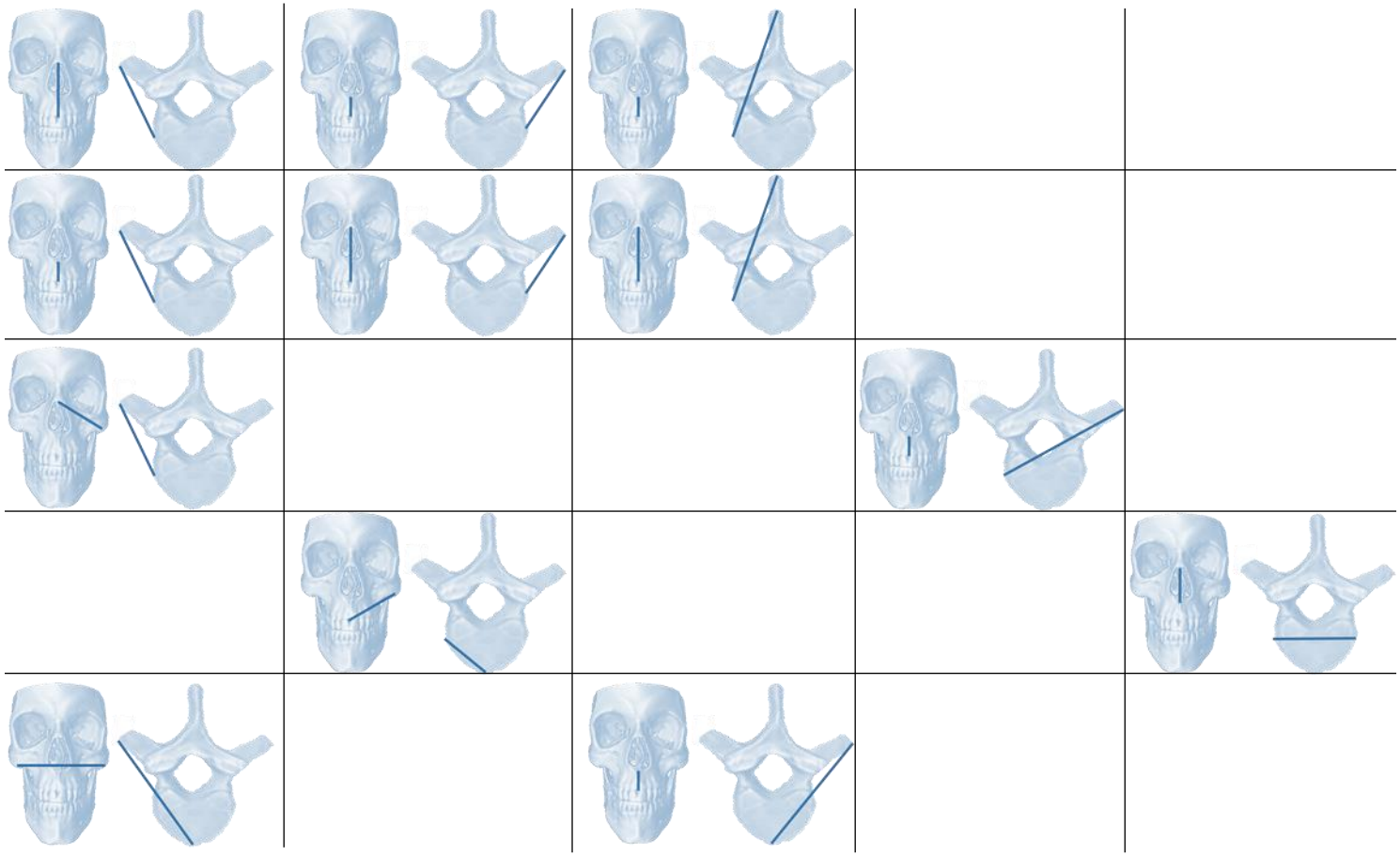

Figure 9: Significant correlation differences are depicted in blue where the original correlation was positive in the kyphosis sample and negative in the control sample. Correlations involving the same linear distance measure from the vertebra are stacked to observe patterns in the results, while others are spaced out.

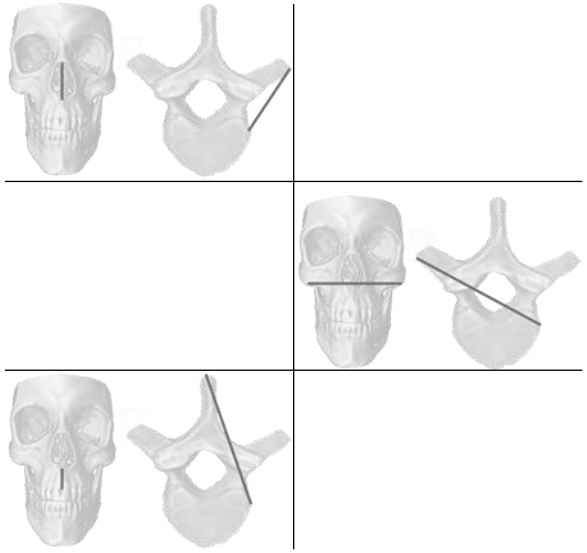

Figure 10: Significant correlation differences are depicted in grey where the original correlation was positive in the kyphosis sample and positive in the control sample. Because none of the positive/positive correlations duplicate a particular vertebra measure, all paired linear distances are spaced out.

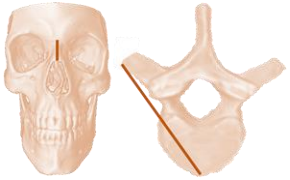

Figure 11: A single significant correlation difference is depicted in red where the original correlation was negative in the kyphosis sample and negative in the control sample.

Correlation Strength Patterns

To explore the absolute strength of the original correlation values from each sample for each significant correlation difference the following absolute correlation classifications were used: absolute value of 0-0.1 very weak, 0.11-0.30 weak, 0.31-0.5 moderate, and 0.51-1.00 strong. Absolute correlation strength differences between samples for those measures that are significantly different were divided as follows: very weak/very weak (n = 1), very weak/moderate (n = 2), very weak/strong (n = 3), weak/weak (n = 1), weak/moderate (n = 10), weak/strong (n = 5), moderate/very weak (n = 3), moderate/weak (n = 3), moderate/moderate (n = 1), strong/very weak (n = 3), and strong/weak (n = 3) (Figure 12, 13, 14, and 15).

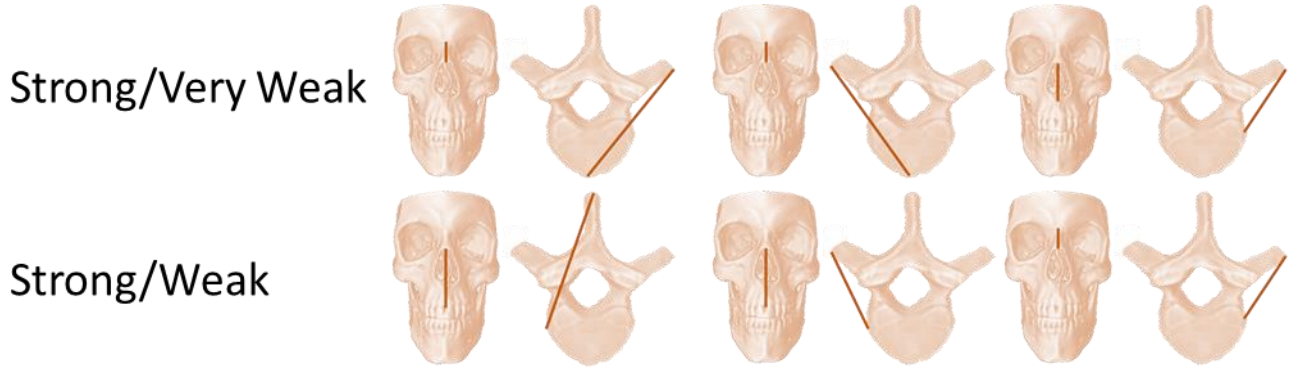

Figure 12: Significant correlation differences are shown where the original kyphosis correlation exhibited strong strength, while the normal correlations were very weak or weak. Kyphosis paired linear distances depicted in red exhibited stronger correlations than corresponding paired linear distances of controls, indicating increased morphological integration for kyphosis measures relative to controls.

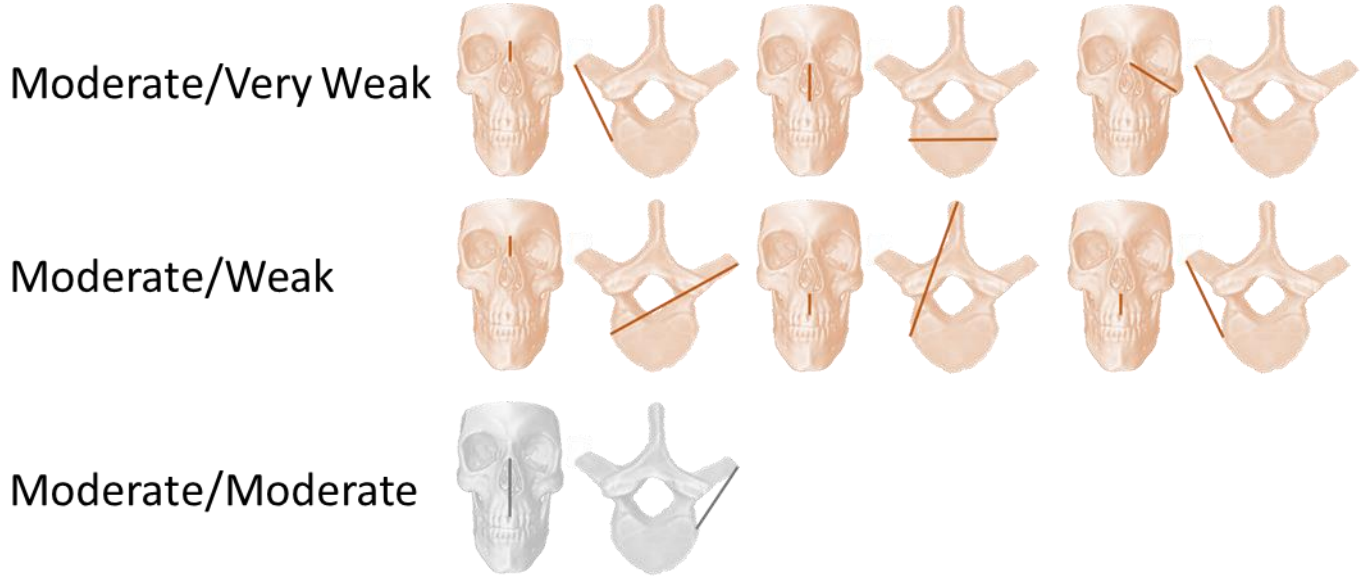

Figure 13: Significant correlation differences are shown where the original kyphosis correlation exhibited moderate strength, while the normal correlations were very weak, weak, or moderate. Kyphosis paired linear distances depicted in red exhibited stronger correlations than corresponding paired linear distances of controls, indicating increased morphological integration for kyphosis measures relative to controls. One pair of linear distances exhibited similar strength in both samples (grey).

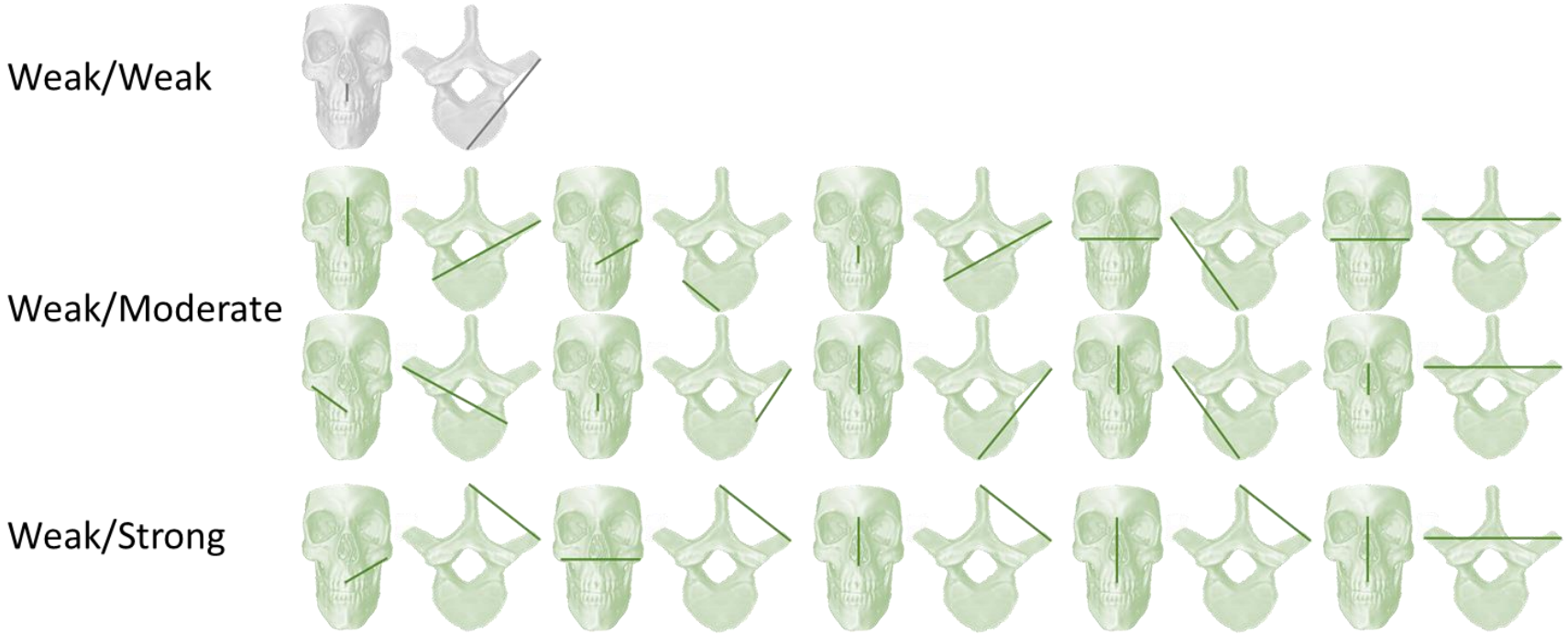

Figure 14: Significant correlation differences are shown where the original kyphosis correlation exhibited weak strength, while the normal correlations were weak, moderate, or strong. Control paired linear distances depicted in green exhibited stronger correlations than corresponding paired linear distances of the kyphosis sample, indicating increased morphological integration for control measures relative to kyphosis measured. One pair of linear distances exhibited similar strength in both samples (grey).

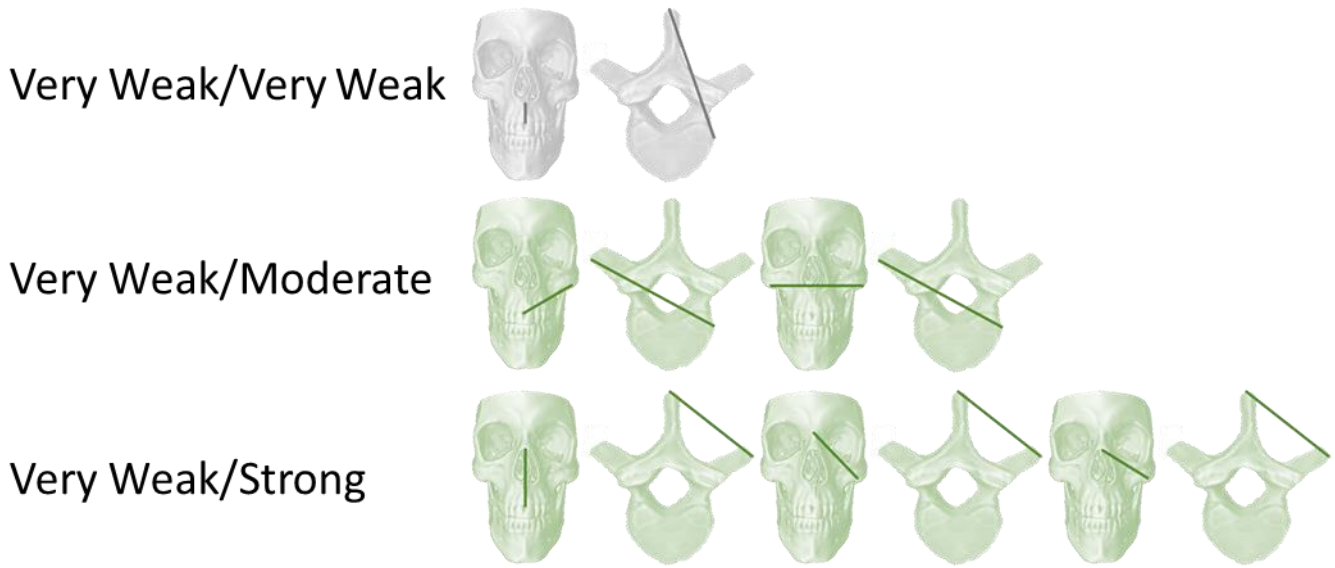

Figure 15: Significant correlation differences are shown where the original kyphosis correlation exhibited very weak strength, while the normal correlations were very weak, moderate, or strong. Control paired linear distances depicted in green exhibited stronger correlations than corresponding paired linear distances of the kyphosis sample, indicating increased morphological integration for control measures relative to kyphosis measures. One pair of linear distances exhibited similar strength in both samples (grey).

Although the patterns are less clear for this interpretative framework relative to the others employed, for 20 of the significant differences (57.1%) the original correlation values exhibit a lower strength in the kyphosis sample and a higher strength in the control sample (i.e., very weak/moderate, very weak/strong, weak/moderate, weak/strong). For 12 of the significant differences (34.3%), the original correlation values exhibit a higher strength in the kyphosis sample and a lower strength in the control sample (i.e., moderate/very weak, moderate/weak, strong/very weak, strong/weak). For the remaining values the correlation strength pattern is the same in each sample (i.e., weak/weak, moderate/moderate). Thus, there is a slight tendency for correlation strengths to be stronger in the control sample, which could be taken as evidence that kyphosis weakens integration among the vertebra and midfacial region of the skull. However, this tendency is tapered by the opposite pattern found in many of the raw correlation values used to calculate significant differences.

Additionally, a summary of absolute correlation strength for each sample is shown in Figure 16. Overall, the control sample is characterized by mostly strong and moderate correlation strengths, while the kyphosis sample is often associated with weak correlation strengths between vertebral and midfacial measurements. Again, this suggests a pattern where kyphosis alters relationships among structures, but this pattern is not consistent.

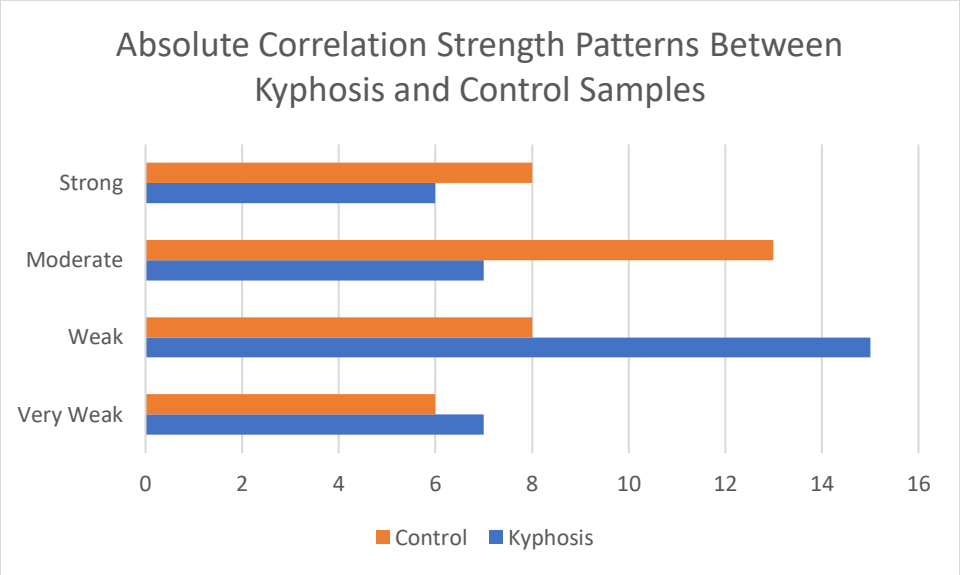

Figure 16: Bar graph summary depicting correlation strength patterns across samples.

Discussion

Overall, relatively few linear distance pairs from the vertebra and midfacial region exhibited a statistically significant difference in correlation values (35 out of 225, or 15.56%), as shown in Figure 3 and Tables 11 and 12. In other words, there are relatively few significant differences in morphological integration when comparing the kyphosis and control samples. This suggests that kyphosis does not have a huge effect on the midfacial region of the skull, although there are some significant differences that can be explored in further detail.

For those 35 linear distance pairs that do significantly differ between samples some pattern differences were discerned. Approximately 60% (21 of 35) of correlation differences exhibit a higher magnitude of integration in the control sample (Figure 4), while 40% (14 or 35) have a higher magnitude of integration in the kyphosis sample (Figure 5). This suggests slightly

less integration in the kyphosis sample overall, which is consistent with the hypothesis that kyphosis weakens integration between vertebrae and the midfacial region of the skull.

Furthermore, the directionality of correlation patterns was explored for those linear distances pairs that significant differ between samples. Interestingly, the kyphosis sample often exhibits a negative correlation, when the control sample exhibits a positive correlation (19 out of 35, or 54%), as shown in Figure 8. In many situations the kyphosis sample exhibited a positive correlation when the control sample exhibited a negative correlation (12 out of 35, or 34%), which is shown in Figure 9. In relatively few situations correlation directionality was positive (3 out of 35, or 9%), as seen in Figure 10, or negative (1 out of 35, or 3%), as seen in Figure 11, in both samples. This tendency for the kyphosis sample to often exhibit a negative correlation when the control sample exhibits a positive correlation also can be taken as evidence that kyphosis influences integration between the T6 vertebra and midfacial region, but this pattern is not consistent across all measures.

Additionally, the comparison of the absolute strength of the original correlation values from each significant difference revealed that kyphosis correlations are usually not absolutely higher than corresponding correlations in the control sample (12 out of 35, or 34%), as shown in Figures 12 and 13. In most situations the original correlation values were absolutely higher in the control sample relative to the kyphosis sample (20 out of 35, or 57%), shown in Figures 13, 14, and 15. Very few absolute correlations exhibited the same strength in both samples (3 out of 35, or 9%), illustrated in Figures 13, 14, and 15. Moreover, a comparison of absolute strength patterns between samples revealed that the control sample is characterized by mostly strong to moderate correlations strengths, while the kyphosis sample often displays weak correlations. The tendency for the control sample to exhibit higher absolute correlation strengths relative to the

kyphosis sample also suggests that integration is affected by kyphosis, but again this pattern is not always consistent.

Based on the results of this study, there are significant correlation differences between the midfacial region of the skull and T6 thoracic vertebrae in individuals with kyphosis and controls. Patterns of integration among those paired measurements that significantly differ between samples often suggest that kyphosis alters patterns of normal integration found in controls, but inconsistency in the direction of these results does not reveal a clear tendency of kyphosis to disrupt integration patterns.

It is important to note that 84.44% of paired linear distance measurements that were tested failed to reach statistical significance. This suggests that kyphosis only has a minor effect on the midfacial region of the skull. Previous studies have suggested multidisciplinary treatment of patients through orthodontic-orthognathic surgeries, as well as more simplistic treatments such as the use of a back brace (Amat, 2009; Ikemitsu et al., 2006). However, it is important to note that these studies detected larger and more differences than this study. This suggests that kyphosis may have a larger effect on the mandible and mandibular teeth, perhaps because the mandible is more mobile as a combined hinge and gliding joint, and therefore more capable of being influenced by spinal deviation over time. While individuals with kyphosis are more prone to possess some form of effect on their midfacial anatomy from their dysmorphic thoracic vertebrae, these effects likely are not strong enough to warrant surgical correction

For biomedical anthropologists, the relatively few significant correlation differences and their associated patterns of integration will likely limit or prevent assumptions about the cultural differences or nuances between kyphosis and non-kyphosis individuals and populations.

Future Research

In order to improve upon this study, there are various approaches that can be put into place in order to ensure more reliable data testing, as well as ensure that the data collected reflects a wide-reaching population rather than possibly isolated cases. These additional steps include improving the research design, such as improving the initial data gathering stage, data testing stage, and data analysis stage, and are outlined below.

Sample Sizes

Future studies of this topic will require larger sample sizes. Larger sample sizes will produce more robust statistical results. For example, if a large sample size yields substantial correlations pattern differences, researchers will be able to assume that these correlation patterns are widespread throughout a population rather than isolated to the relatively few cases assessed in this preliminary investigation.

Regarding the control sample, future research should be sure to examine the range of variation among individuals. One aspect to consider in control samples is any possible cases of asymmetry in the musculoskeletal anatomy. While not conclusive, past studies have shown that asymmetry can arise due to habitual high-impact gravitational loads, which is common in athletics and certain occupations (Hart, 2016 & Evershed, 2014). Prior to determining a concrete control sample, it would be beneficial to consider health behaviors or the work environments of individuals to try and control for musculoskeletal asymmetry.

For future studies it could be beneficial to place individuals into sample sizes that correlate to ethnicity. While the sample size for this study was small enough to where ethnicity would not have major outcomes on the data outcomes, it may be beneficial for future research to

incorporate groupings that separate between ethnicities. This is due to the nature of human variation between ethnicities of modern human populations. One example of this variation is found in the degree of prognathism across different ethnicities. Previous studies have found that the gnathic index (the degree of relative protrusion of the jaw) can differ among geographically distance human populations, such as African and European populations (Lesicotto, et al., 2016). This variation between populations differs enough to where it may alter morphological integration of the thoracic vertebrae and the midfacial region of the skull. Separate groups for respective ethnicities will allow researchers to not only better examine the effects of morphological integration between ethnic groups but may also allow researchers to gain an understanding of how variation may effect morphological integration of the thoracic vertebrae and midfacial region of the skull.

Dividing individuals with kyphosis and individuals without kyphosis into distinctive age groups may also greatly improve the understanding of morphological integration of the thoracic vertebrae and midfacial region of the skull. Weakened bones are commonly associated with older individuals, but younger individuals may also have weakened bones stemming from osteoporosis or other pathological influences. As mentioned in the introduction, weakened bone strength can cause the wedging and wearing away of thoracic vertebrae which leads to degrees of kyphosis in the vertebral column. In addition to studying the effects kyphosis has on biological processes, dividing individuals into distinct age groupings can allow future studies to observe any possible differences in health behaviors or cultural patterns between generations. In the control sample, age-based groupings in addition to attempts to control variation between individuals will allow researchers to further examine the relation of weakened bone strength relative to causations of kyphosis. While not all older individuals have kyphosis, they will have varying degrees of

weakened bone strength as a result of the human aging process. Perhaps distinctions in age groupings can also open up new viewpoints for research, specifically on how bone strength has the potential to effect morphological integration.

It would also be beneficial in future studies for samples to be further divided. Rather than simply divide individuals into two groups of either "Kyphosis" or "Control", it could be beneficial to separate individuals with kyphosis into groups of severe or mild cases or even more subdivisions. Like most status ailments, kyphosis appears in humans to differing degrees. By further dividing individuals exhibiting signs of kyphosis, researchers will be able to gather more detailed results as to how different degrees of kyphosis in the vertebral column can affect other anatomical regions of the human body. It is hypothesized that severe cases of kyphosis will be much more likely to disrupt patterns of morphological integration than mild cases. It may also be beneficial to divide congenital cases in which kyphosis is still present in adults. Congenital cases are more likely to be more severe and have the potential to greatly effect data outcome and assessment (Zhang, 2017). While no current studies focusing on the midfacial region of the human skull have taken this approach, it has been used in studies focusing on the effects of spinal malformations on dental morphology. Previous studies have further divided samples into groups based upon the degree of dental malocclusion exhibited, such as Class I or Class II (Saccuci et al., 2011).

Regarding the control sample, future research should be sure to examine the range of variation among individuals. One aspect to consider in control samples is any possible cases of asymmetry in the musculoskeletal anatomy. While not conclusive, past studies have shown that asymmetry can arise due to habitual high-impact gravitational loads, which is common in athletics and certain occupations (Hart, 2016 & Evershed, 2014). While considering overall

asymmetry, it is also important to consider the more naturally occurring asymmetry among the maxillary provenience (i.e. the midfacial region of the skull). Physical anthropological research in the past has shown that the maxillary sinus process is prone to high variability possibly due to factionary senses, thermoregulation, or masticatory stresses (Butaric, 2010). While the main reason for this asymmetry is not conclusive, it is a variable to consider while conducting future research on morphological integration. While the maxillary provenience is more likely to exhibit asymmetry due to natural occurrences, vertebrae are prone to change from environmental factors, including minor cultural norms such as habitual use of carrying a backpack, present in most current-day societies (Drzał-Grabiec, 2015). Prior to determining a concrete control sample, it would be beneficial to consider health behaviors, work environment, and cultural upbringing of individuals to try and control for overall asymmetry, as well as asymmetry specific to the midfacial region and vertebrae.

Additional Landmarks

For future research it will be quite beneficial for researchers to incorporate additional landmark measurements while studying CT images of the skull and vertebral column of individuals with kyphosis. Additional landmarks will allow for a larger number of linear distance measurements to be studied, which in turn will allow for a greater amount of statistical correlations to be observed. While landmarks in this study mainly focus on the left and right zygomaxillare and the nasomaxillary anatomy of the midfacial region of the skull, additional landmarks could be added to anatomical structures such as the left and right supraorbital notches, the left and right infraorbital foramen, and along the optic canal to name a few. Anatomical

structures of the skull outside of the midfacial region could also be studied in addition to the midfacial region. Studying other regions of the skull may produce interesting results as well.

Future studies will also benefit from an increased number of landmarks along the vertebrae as well. For this study, landmarks were placed mainly on the superior transverse process as well as the superior border of the vertebral body. However, only one landmark was placed on the posterior anatomy of the vertebrae, that of the spinous process. The chosen landmarks allowed the calculation of length and width measured, but failed to assess vertebral height, which can be affected by kyphosis and age. Future research, with a longer research timeline than that afforded to HIM research, could benefit from adding additional landmarks to posterior anatomical features, such as the lamina, mammillary process, or the inferior articular process.

Measurement Error

A decrease in measurement error in the overall landmarking of individuals will also be highly beneficial for future research. There is a learning curve to identifying and placing anatomical landmarks on 3D volume renderings and 2D orthoslices from CT images. While twenty-four hours passed in between the first and second trials of landmarking individuals to prevent memory bias, increasing the amount of trials could help reduce the amount of measurement error between trials by implementing better practice and consistency of landmarking by the researcher. While the overall amount of measurement error was low between trials, some high measurement errors were still present. Through an increase in the amount of trials conducted, the researcher placing landmark measurements will have greater practice in placing the specific landmarks, which could result in lower overall measurement error.

Conclusions

Overall, there is much to do concerning the improvement of future research. Regarding the data gathered from this research, the relatively few significant correlation differences and their associated patterns of integration will likely limit or prevent assumptions about the cultural differences or nuances between kyphosis and non-kyphosis individuals and populations. While a lack of significant difference correlations may indicate a lack of difference in health behaviors between kyphotic and non-kyphotic individuals, future research would greatly benefit from having a better understanding of these behaviors prior to the landmarking process of anatomical structures. This includes not only previous health history, but also to consider the cultural factors that may influence any health behaviors present.

References

Amat, P. "Occlusion, Orthodontics and posture: are there evidences? The example of scoliosis." *International Journal of Stomatology and Occlusion Medicine*, vol. 2, no. 1, 2009, pp. 2-10.

Benzel, Edward, Stillerman, Charles. *The Thoracic Spine*. (Stuttgart: Thieme Medical Publishers), 1994.

Butaric, N. Lauren, McCarthy, C. Robert, Broadfield, C. Douglas. "A preliminary 3D computed tomography study of the human maxillary sinus and nasal cavity." *American Journal of Physical Anthropology*, vol.143, no.3, 2010.

Cole TM III, Lele S. Bootstrap-based methods for comparing morphological integration patterns. *Am J Phys Anthropology*, vol. 117, no. 34, 2002, pp. 55.

Drzal-Grabiec, Justyna, Rachwal, Maciej, Podgorska, Justyna, Rykala, Justyna, Snela, Slawomir. "Effects of Carrying a Backpack in an Asymmetrical Manner on the Asymmetries of the Trunk and Parameters Defining Lateral Flexion of the Spine." *Human Factors*, vol. 57, no.2, 2015, pp. 218-226.

Evershed, Jo, Burkett, Brendan, Mellifont, Rebecca. "Musculoskeletal screening to detect asymmetry in swimming." *Physical Therapy in Sport*, vol.15, no.1, 2014, pp. 33-39.

Harrison, A. Robyn, Simonski, Kerry, Vethanayagam, Dilini, Majumdar, R. Sumit. "Osteoporosis-Related Kyphosis and Impairments in Pulmonary Function: A Systematic Review." *Journal of Bone & Mineral Research*, vol.22, no.3, 2007, pp. 447-458.

Hart, H. Nicolas, Nimphius, Sophia, Weber, Jason, Spiteri, Tania, Rantalainen, Timo, Dobbin, Michael, Newton, U. Robert. "Musculoskeletal Asymmetry in Football Athletes: A product of Limb Function over Time." *Medicine & Science in Sports & Exercise*, vol. 48, no.7, 2016, pp. 1379-1388.

Hooker, Karen, Mejia, Shannon, Ram, Nilam, Pham, Tuan, Metoyer, Ron. "Capturing Intraindividual Variation and Covariation Constructs: Using Multiple Time-Scales to Assess Construct Reliability and Construct Stability." *Research in Human Development*, vol.11, no.2, 2014, pp. 97-107.

Huggare, Jan. "Postural disorders and dentofacial morphology." *Acta Odontologica Scandinavia*, vol. 56, no. 6, 1998, pp. 383-386.

Ikemitsu, Himiko, Zeze, Ryousuke, Yuasa, Kenji, Izumi, Kiwako. "The relationship between jaw deformity and scoliosis." *Oral Radiology*, vol. 22, no.1, 2006, pp. 14-17.

Jain, K., Anil, Dhammi, Kumar Ish, Jain, Saurabh, Mishra, Puneet. "Kyphosis in spinal tuberculosis – Prevention and correction." *Indian Journal of Orthopaedics*, vol. 44, no.2, 2010, pp. 127-136.

Johnston, E. Francis, Low, M. Setha. "Biomedical Anthropology: An Emerging Synthesis in Anthropology." *Yearbook of Physical Anthropology*, vol. 27, 1984, 215-227.

Klingenberg, Christian. "Morphological Integration and Developmental Modularity." *Annual Review of Ecology, Evolution, and Systematics*, 2008, pp. 115-128.

Lesciotto, K.M, Cabo, L.L., Garvin, H.M. “A morphometric analysis of prognathism and evaluation of the gnathic index in modern humans.” *Journal of Comparative Human Biology*, vol.67, 2016, pp. 294-312.

Lippold, Carsten, Danesha, Gholmareza, Hoppeb, Glorida, Drerupc, Burkhard, Hackenbergd, Lars. “Relationship between Thoracic, Lordotic, and Pelvic Inclination and Craniofacial Morphology in Adults.” *Angle Orthodontics*, vol. 76, no.5, 2006, pp. 779-785.

Olson, C. Everett, Miller, L. Robert. *Morphological Integration*. (Chicago: Chicago University Press), 1958.

Richtsmeier, J.T., Aldridge, K, DeLeon, VB, Panchal, J, Kane, A.A., Marsh, J.L., Yan, P, Cole, T.M. III. Phenotypic integration of neurocranium and brain. *J Exp Zool B Mol Dev Evol* vol. 306, vol. 4, 2006, pp. 360–378.

Richtsmeier, J.T., DeLeon, V.B. Morphological integration of the skull in craniofacial anomalies. *Orthod Craniofac Res* vol. 12, no.3, 2009, pp. 149–158.

Richtsmeier J.T., Lele, S. *An Invariant Approach to Statistical Analysis of Shapes*. (Florida: Chapman and Hall/CRC Press), 2001.

Saccucci, Matteo, Tettamanti, Lucia, Mummolo, Stefano, Polimeni, Antonella, Festa, Felice, Salini, Vincenzo, Tecco, Simona. “Scoliosis and dental occlusion: a review of the literature.” *Scoliosis Journal*, vol.6, no.15, 2011.

Starbuck, J, Reeves, R., Richtsmeier, J. “Morphological Integration of Soft-Tissue Facial Morphology in Down Syndrome and Siblings.” *American Journal of Physical Anthropology*, vol. 146, 2011, pp. 560-568.

Tribus, B. Clifford. "Scheuermann's Kyphosis in Adolescents and Adults: Diagnosis and Management," *Journal of the American Academy of Orthopaedic Surgeons*, vol. 6, 1998, pp. 36-43.

Vaughan, L. Christopher. "Theories of bipedal walking: an odyssey." *Journal of Biomechanics*, vol. 36, no. 4, 2003, pp. 513-523.

Wippert, Maria, Rector, Michael, Kuhn, Gisela, Wuetz-Kozak, Karin. "Stress and Alterations in Bones: An Interdisciplinary Perspective." *Front Endocrinol (Lausanne)*, vol. 8, 2017, pp. 96.

Zhang, Zhengfeng, Wang, Honggang, Zheng, Wenjie. "Compressive Myelopathy in Congenital Kyphosis of the Upper Thoracic Spine: A Retrospective Study." *Clinical Spine Surgery*, vol. 38, no. 8, 2017, pp. 1098 – 1103.